Modelling suspended sediment transport on Australia's North West Shelf

NWSJEMS

TECHNICAL REPORT No. 7

- N. Margvelashvili • J. Andrewartha • S. Condie
- M. Herzfeld • J. Parslow • P. Sakov • J. Waring

June 2006

CSIRO

GOVERNMENT OF WESTERN AUSTRALIA

Department of
Environment

NORTH WEST SHELF JOINT ENVIRONMENTAL MANAGEMENT STUDY

Final report

North West Shelf Joint Environmental Management Study Final Report.

List of technical reports

NWSJEMS Technical Report No. 1
Review of research and data relevant to marine environmental management of Australia's North West Shelf.
A. Heyward, A. Revill and C. Sherwood

NWSJEMS Technical Report No. 2
Bibliography of research and data relevant to marine environmental management of Australia's North West Shelf.
P. Jernakoff, L. Scott, A. Heyward, A. Revill and C. Sherwood

NWSJEMS Technical Report No. 3
Summary of international conventions, Commonwealth and State legislation and other instruments affecting marine resource allocation, use, conservation and environmental protection on the North West Shelf of Australia.
D. Gordon

NWSJEMS Technical Report No. 4
Information access and inquiry.
P. Brodie and M. Fuller

NWSJEMS Technical Report No. 5
Data warehouse and metadata holdings relevant to Australia's North West Shelf.
P. Brodie, M. Fuller, T. Rees and L. Wilkes

NWSJEMS Technical Report No. 6
Modelling circulation and connectivity on Australia's North West Shelf.
S. Condie, J. Andrewartha, J. Mansbridge and J. Waring

NWSJEMS Technical Report No. 7
Modelling suspended sediment transport on Australia's North West Shelf.
N. Margvelashvili, J. Andrewartha, S. Condie, M. Herzfeld, J. Parslow, P. Sakov and J. Waring

NWSJEMS Technical Report No. 8
Biogeochemical modelling on Australia's North West Shelf.
M. Herzfeld, J. Parslow, P. Sakov and J. Andrewartha

NWSJEMS Technical Report No. 9
Trophic webs and modelling of Australia's North West Shelf.
C. Bulman

NWSJEMS Technical Report No. 10
The spatial distribution of commercial fishery production on Australia's North West Shelf.
F. Althaus, K. Woolley, X. He, P. Stephenson and R. Little

NWSJEMS Technical Report No. 11
Benthic habitat dynamics and models on Australia's North West Shelf.
E. Fulton, B. Hatfield, F. Althaus and K. Sainsbury

NWSJEMS Technical Report No. 12
Ecosystem characterisation of Australia's North West Shelf.
V. Lyne, M. Fuller, P. Last, A. Butler, M. Martin and R. Scott

NWSJEMS Technical Report No. 13
Contaminants on Australia's North West Shelf: sources, impacts, pathways and effects.
C. Fandry, A. Revill, K. Wenziker, K. McAlpine, S. Apte, R. Masini and K. Hillman

NWSJEMS Technical Report No. 14
Management strategy evaluation results and discussion for Australia's North West Shelf.
R. Little, E. Fulton, R. Gray, D. Hayes, V. Lyne, R. Scott, K. Sainsbury and D. McDonald

NWSJEMS Technical Report No. 15
Management strategy evaluation specification for Australia's North West Shelf.
E. Fulton, K. Sainsbury, D. Hayes, V. Lyne, R. Little, M. Fuller, S. Condie, R. Gray, R. Scott,
H. Webb, B. Hatfield, M. Martin, and D. McDonald

NWSJEMS Technical Report No. 16
Ecosystem model specification within an agent based framework.
R. Gray, E. Fulton, R. Little and R. Scott

NWSJEMS Technical Report No. 17
Management strategy evaluations for multiple use management of Australia's North West Shelf
– Visualisation software and user guide.
B. Hatfield, L. Thomas and R. Scott

NWSJEMS Technical Report No. 18
Background quality for coastal marine waters of the North West Shelf, Western Australia.
K. Wenziker, K. McAlpine, S. Apte, R.Masini

CONTENTS

ACRONYMS

ACOM	Australian Community Ocean Model
AFMA	Australian Fisheries Management Authority
AFZ	Australian Fishing Zone
AGSO	Australian Geological Survey Organisation now Geoscience Australia
AHC	Australian Heritage Commission
AIMS	Australian Institute of Marine Science
AMSA	Australian Maritime Safety Authority
ANCA	Australian Nature Conservation Agency
ANZECC	Australian and New Zealand Environment and Conservation Council
ANZLIC	Australian and New Zealand Land Information Council
APPEA	Australian Petroleum, Production and Exploration Association
AQIA	Australian Quarantine Inspection Service
ARMCANZ	Agricultural Resources Management council of Australia and New Zealand
ASIC	Australian Seafood Industry Council
ASDD	Australian Spatial Data Directory
CAAB	Codes for Australian Aquatic Biota
CAES	Catch and Effort Statistics
CALM	Department of Conservation and Land Management (WA Government)
CAMBA	China Australia Migratory Birds Agreement
CDF	Common data format
CITIES	Convention on International Trade in Endangered Species
CTD	conductivity-temperature-depth
CMAR	CSIRO Marine and Atmospheric Research
CMR	CSIRO Marine Research
COAG	Council of Australian Governments
ConnIe	Connectivity Interface
CPUE	Catch per unit effort
CSIRO	Commonwealth Science and Industrial Research Organisation
DCA	detrended correspondence analysis
DIC	Dissolved inorganic carbon
DISR	Department of Industry, Science and Resources (Commonwealth)
DEP	Department of Environmental Protection (WA Government)
DOM	Dissolved organic matter
DPIE	Department of Primary Industries and Energy
DRD	Department of Resources Development (WA Government)
EA	Environment Australia
EEZ	Exclusive Economic Zone
EIA	Environmental Impact Assessment
EPA	Environmental Protection Agency
EPP	Environmental Protection Policy
ENSO	El Nino Southern Oscillation
EQC	Environmental Quality Criteria (Western Australia)
EQO	Environmental Quality Objective (Western Australia)
ESD	Ecologically Sustainable Development
FRDC	Fisheries Research and Development Corporation
FRMA	Fish Resources Management Act
GA	Geoscience Australia formerly AGSO
GESAMP	Joint Group of Experts on Scientific Aspects of Environmental Protection
GIS	Geographic Information System
ICESD	Intergovernmental Committee on Ecologically Sustainable Development
ICS	International Chamber of Shipping
IOC	International Oceanographic Commission
IGAE	Intergovernmental Agreement on the Environment
ICOMOS	International Council for Monuments and Sites
IMO	International Maritime Organisation

IPCC	Intergovernmental Panel on Climate Change
IUNC	International Union for Conservation of Nature and Natural Resources
IWC	International Whaling Commission
JAMBA	Japan Australian Migratory Birds Agreement
LNG	Liquified natural gas
MarLIN	Marine Laboratories Information Network
MARPOL	International Convention for the Prevention of Pollution from Ships
MECO	Model of Estuaries and Coastal Oceans
MOU	Memorandum of Understanding
MPAs	Marine Protected Areas
MEMS	Marine Environmental Management Study
MSE	Management Strategy Evaluation
NCEP - NCAR	National Centre for Environmental Prediction – National Centre for Atmospheric Research
NEPC	National Environmental Protection Council
NEPM	National Environment Protection Measures
NGOs	Non government organisations
NRSMPA	National Representative System of Marine Protected Areas
NWQMS	National Water Quality Management Strategy
NWS	North West Shelf
NWSJEMS	North West Shelf Joint Environmental Management Study
NWSMEMS	North West Shelf Marine Environmental Management Study
ICIMF	Oil Company International Marine Forum
OCS	Offshore Constitutional Settlement
PFW	Produced formation water
P(SL)A	Petroleum (Submerged Lands) Act
PSU	Practical salinity units
SeaWiFS	Sea-viewing Wide Field-of-view Sensor
SOI	Southern Oscillation Index
SMCWS	Southern Metropolitan Coastal Waters Study (Western Australia)
TBT	Tributyl Tin
UNCED	United Nations Conference on Environment and Development
UNCLOS	United Nations Convention of the Law of the Sea
UNEP	United Nations Environment Program
UNESCO	United Nations Environment, Social and Cultural Organisation
UNFCCC	United Nations Framework Convention on Climate Change
WADEP	Western Australian Department of Environmental Protection
WADME	Western Australian Department of Minerals and Energy
WAEPA	Western Australian Environmental Protection Authority
WALIS	Western Australian Land Information System
WAPC	Western Australian Planning Commission
WHC	World Heritage Commission
WOD	World Ocean Database
www	world wide web

TECHNICAL SUMMARY

The distributions and movements of sediments on the North West Shelf have a major influence on the ecosystem, primarily through their effect on primary production and benthic habitat distributions. They are also highly relevant to human activities on the NWS, particularly construction and maintenance of offshore structures, dredging, and other coastal developments involving habitat modification.

This study provides a general characterisation of the distributions of suspended and bottom sediments based on available data. These data confirm the existence of a high turbidity zone extending from the coastline to around the 20 m isobath. Bottom sediments also show a marked cross shelf zonation, with gravel and sand dominating the inner shelf, and finer sand, silts and clays dominating the less energetic outer shelf.

A three dimensional sediment transport model was developed to estimate major resuspension, deposition, and suspended transport patterns over the NWS. The simulations covered the three years 1996, 1998, and 1999. They successfully reproduced the winnowing of fine sediments (i.e. very fine sand, silts and clays) in the relatively high-energy environment of the mid shelf, and their subsequent export onto the continental slope. The model also predicted a persistent strip of elevated suspended sediment concentrations along the inner shelf. Near surface suspended sediment concentrations in this zone typically increased by an order of magnitude from the neap to spring tide. Long-termed average sediment fluxes were directed southwest along the shelf and off the shelf. While there were significant uncertainties associated with these fluxes, the results suggested that sediment losses from the shelf exceeded the mean annual river loads by at least a factor of three over the simulation period.

The model also predicted major sediment transport events during tropical cyclones. Modelled off shelf loads during Tropical Cyclone Bobby far exceeded both annual river loads and annual loads during non-cyclone conditions. These simulations also demonstrated how cyclone induced ocean eddies could capture large quantities of suspended sediments and carry them offshore to be deposited within highly localised patches in the deeper ocean.

While there were various limitations in the model formulation, its predictions were broadly consistent with the limited available observations. It is suggested that further progress in sediment modelling on the NWS should be based on extended data sets for sediment processes, such as grain size distributions, flocculation, consolidation, and river loads, as well as improved wind and wave products, and inclusion of bedload transport.

1.   INTRODUCTION

The North West Shelf Joint Environmental Management Study (NWSJEMS) was aimed at developing the science-based methods required to support integrated regional planning and management of the North West Shelf (NWS) marine environment and resources. A major component of the study was directed at understanding the links between the physical, chemical and biological environments, and predicting ecosystem responses to natural and anthropogenic variability.

A particularly important component of the NWS ecosystem is the distribution and movements of sediments. They have a very strong influence on primary production in the water column and on the seabed, and the distribution and evolution of benthic habitats. Sediments are also of direct interest to many industries operating on the NWS, particularly those concerned with the dispersion of particulate bound contaminants, the impacts of coastal operations such as dredging and other habitat modification, or the stability of offshore structures vulnerable to seabed scouring.

The objectives of the sediment transport task were to characterise the observed bottom sediment distributions and turbidity on the NWS, then develop models to estimate probable resuspension, deposition, and transport patterns. This report describes the spatial and temporal characteristics of sediment transport based on the first attempt to develop a three dimensional coupled hydrodynamic-sediment model of the NWS.

Chapter 2 gives a brief overview of the physical environment on the NWS, including available information on the sediment composition and distributions. In Chapter 3, the sediment transport model is described, including its assumptions, inputs and outputs. Chapter 4 presents and discusses model results, before a summary of the work is presented in Chapter 5. The impacts of sediment movements on biological communities and human activities are described in accompanying reports.

2.   THE PHYSICAL ENVIRONMENT

2.1   Climate and circulation

The NWS study region runs from North West Cape to the Port Hedland region, over which the shelf width increases from less than 20 km to almost 200 km (figure 2.1.1). It is a tropical arid region with a mean annual rainfall of around 300 mm, most of which falls over summer and autumn (Lough, 1998). River flows also peak in summer, but are generally very low. The prevailing summer winds are from the northwest and southwest, swinging around to dry southeasterlies over winter. However, in coastal areas local sea breezes often dominate the daily patterns. Wind waves on the mid and inner shelf are observed to be strongly dependent on local winds, although swell generated by weather systems to the southwest of the region can encroach onto the NWS (Semeniuk et al. 1982; Hamilton, 1997).

During the summer period, tropical cyclones form between northern Australia and Indonesia. An average of two to three a year follow a southwesterley course parallel to the NWS before swinging south and crossing the Pilbara coast. During these events winds can reach 180 km per hour, with extreme downpours, river flooding, and ocean wave heights sometimes exceeding 17 m. Not surprisingly, cyclones can also have a major impact on sediment distributions through both increased river loads and enhanced resuspension rates.

Circulation on the NWS is influenced by the broader scale circulation of the Indonesian Throughflow to the north (Cresswell et al. 1993) and Leeuwin Current to the west (Godfrey & Ridgway, 1985). However, daily current patterns on the NWS tend to be strongly dominated by tidal motions, with semidiurnal flows up to 1 m s^{-1} and tidal ranges up to 6 m on the Pilbara coast (Holloway, 1995). These motions are predominantly in the cross shelf direction, except around Barrow Island and the Monte Bello Islands where they are orientated closer to the east-west direction. Near the shelf break they also generate large nonlinear internal tides, which may intensify bottom flow and vertical mixing rates (Holloway, 1985). Wind forced currents only become dominant around the neap tide, when the main sub-inertial motions are continental shelf waves (Webster, 1985; Holloway & Nye, 1985) and during tropical cyclones when surface current speeds can exceed 3 m s^{-1}.

Various models have been developed to describe tidal motions on the NWS, including primitive equation solutions over a cross shelf section (Holloway, 1996) and fully three dimensional (Holloway, 2001). The cross shelf model has also been extended to include sediment responses to barotropic and internal tides (Ribbe & Holloway, 2001). Other models have been directed at understanding the ocean response to tropical cyclones (Hearn & Holloway, 1990; Fandry & Steedman, 1994). However, NWSJEMS is the first attempt to include sediment processes in a three dimensional model of the region with realistic forcing.
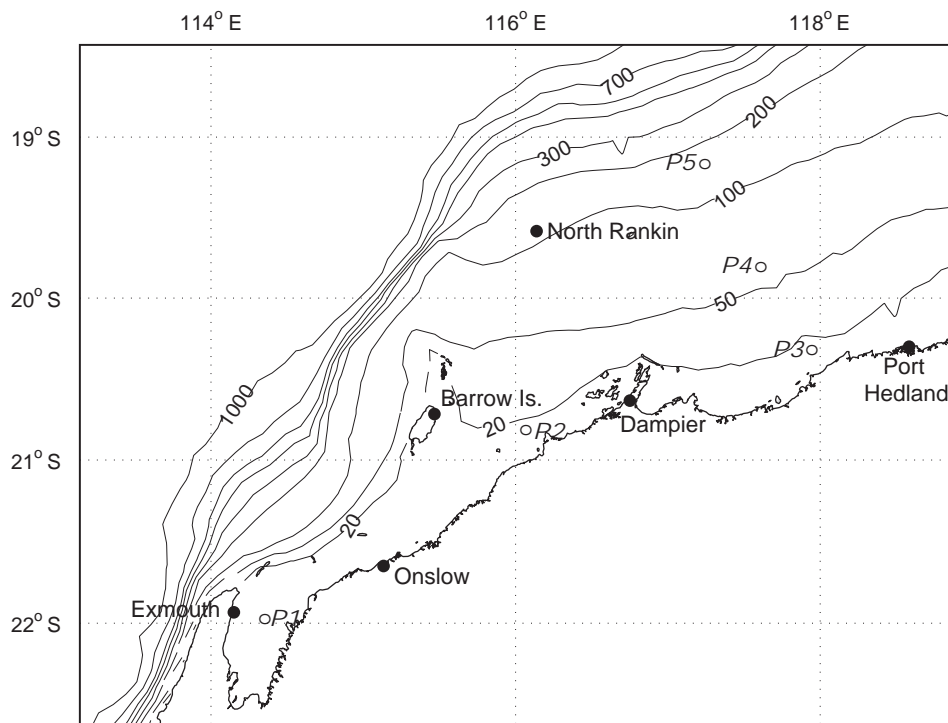
Figure 2.1.1: Bathymetry map of the Pilbara shelf region. Sites P1 to P5 were used for detailed time series analysis of the model outputs.
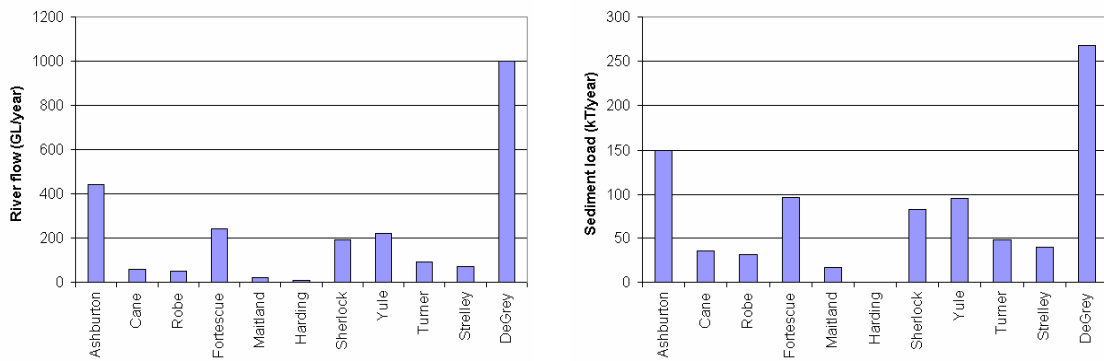
2.2   Suspended sediment

General patterns of turbidity on the NWS can be approximated using satellite ocean colour data. Long-term average turbidity estimates shows a relatively thin turbidity maximum along the inner shelf, which peaks on the eastern side of the mouth of Exmouth Gulf, then gradually declines to the northeast (figure 2.2.1). Such a feature is typical of many shelf seas and can usually be attributed to resuspension by tidal currents (Drake, 1977). The rivers in the Pilbara region flow only occasionally (Ruprecht & Ivansecu, 1996) and under average conditions contribute little to marine turbidity levels (figure 2.2.2). However, turbidity increases with river-flow and flood events can produce extremely turbid conditions on the inner shelf.
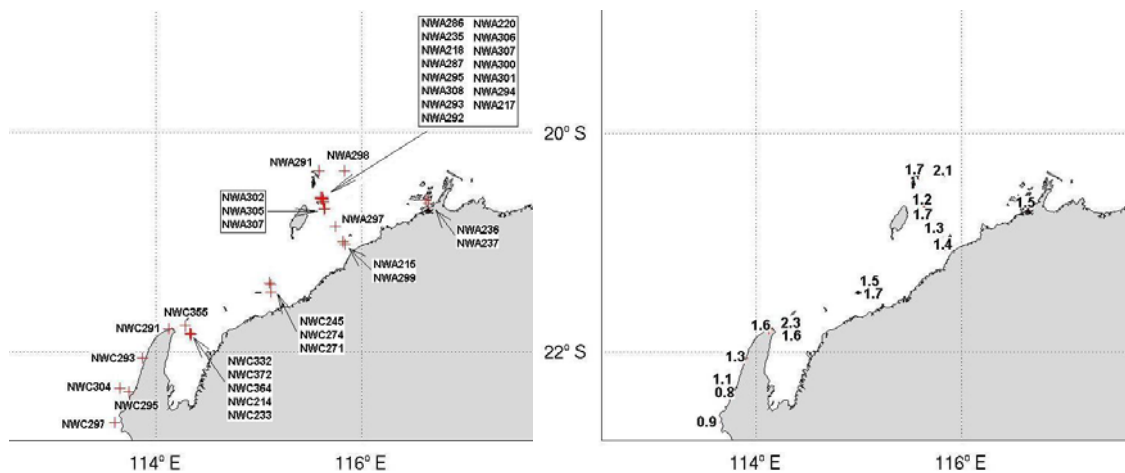
In situ suspended sediment concentrations collected by the Australian Institute of Marine Sciences covered a range of meteorological and hydrological conditions, including wind speeds from 5 to 20 m s^{-1} and swell heights from 0.1 to 2.0 m (figure 2.2.3). They revealed that concentrations tended to increase with depth, although subsurface maxima were not uncommon (figure 2.2.4). Maximum concentrations did not exceed 2.5 g m^{-3} at the surface or 5 g m^{-3} at depth. The data did not show any systematic variation along the shelf. Sediment trap estimates of vertical sediment fluxes have been reported in the range 322 to 616 mg m^{-2} day^{-1} over the outer shelf and slope north of Exmouth Gulf, falling to 124 mg m^{-2} day^{-1} further offshore (Burns et al. 2003).
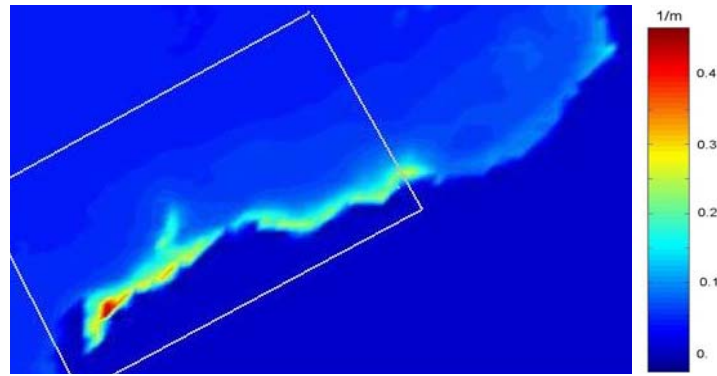
Figure 2.2.1: Mean turbidity on the NWS (1998 to 2000) based on the *SeaWiFS* diffuse attenuation coefficient at wavelength 490 nm (m^{-1}). Standard *SeaWiFS* algorithms based mainly on Northern Hemisphere oceanic measurements have been used, so significant errors are likely on the inner shelf (*SeaWiFS* Technical Report, 1997). The box indicates the area of the model.

Figure 2.2.2: Estimates of mean annual flow (left) and sediment load (right) to the NWS from Pilbara Rivers (Ruprecht & Ivansecu, 1996).


Figure 2.2.3: Location map and identification numbers for suspended sediment concentration measurements (left) and mean surface values in mg L^{-1} (right). The measurements were made by the Australian Institute of Marine Sciences during 9 to 13 September 1994, 18 to 29 September 1995, and November 1998 to February 1999.
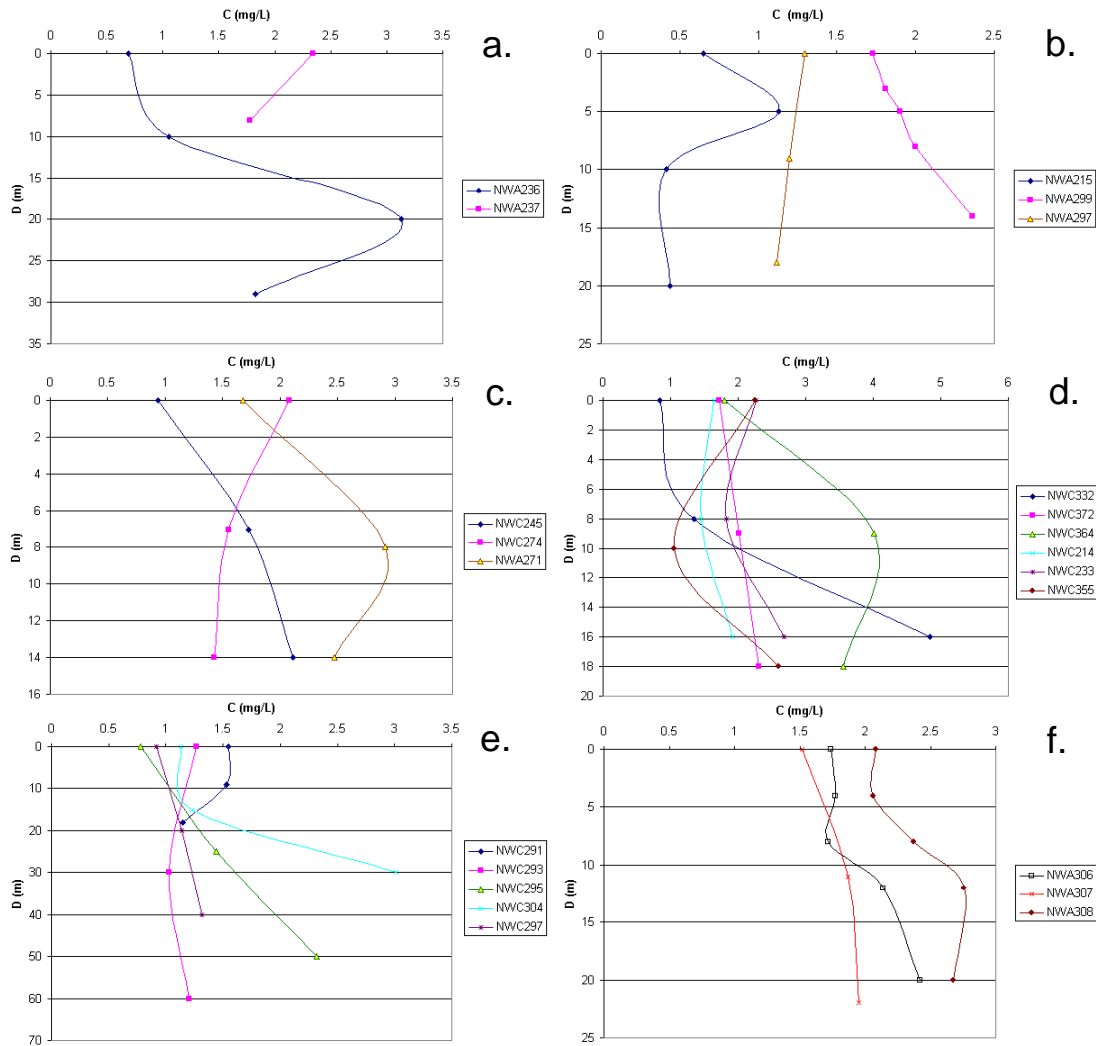
Figure 2.2.4: Suspended particulate concentrations measured on the NWS as a function of depth. Plots (a) to (e) are ordered to show sediment profiles over the inner shelf moving from northeast to southwest, while (f) is near Barrow Island offshore of (b).

2.3   Bottom sediment

Spatial distributions of different sediment classes on the shelf were studied during CSIRO fisheries research cruises prior to 1980 (McLoughlin, 1981; McLoughlin & Young, 1985). Sediment samples were taken at 10 km intervals on a grid covering the shelf between Dampier and Port Hedland within a depth range of 20 to 150 m (figure 2.3.1 (a)). Samples were treated to obtain the grain size spectrum ranging from -1.75 to 14 phi-size with 0.25 phi resolution for gravel and silt fractions, and 1.0 phi resolution for the silt and clay classes (phi = $-\log_2[D]$ where D is grain diameter in mm). These data have been grouped and averaged to represent gravel, sand, silt and clay fractions, before being linearly interpolated onto a uniform grid using the Delaunay triangulation method (figure 2.3.1).
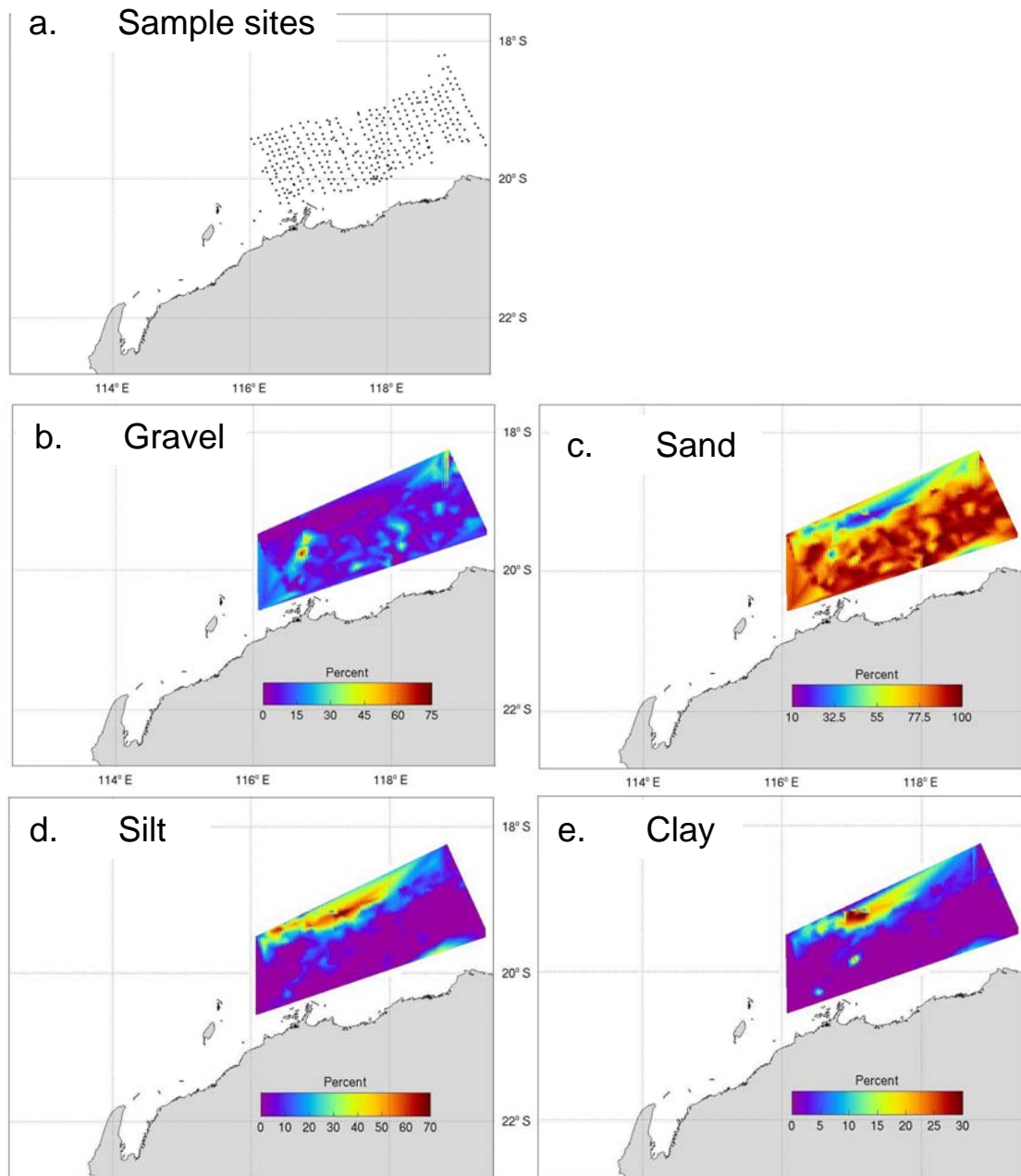
Figure 2.3.1: Distribution of (a) CSIRO bottom sediment sampling sites, (b) gravel, (c) sand, (d) silt, and (e) clay on part of the NWS.

The sediment bed texture changes markedly across the NWS. In the relatively high-energy environment of the mid shelf region, winnowing and transportation leads to high concentrations of gravel and sand fractions. The distributions of these fractions are also characterised by numerous small scale structures, some of which can be attributed to distinct topographical features. For example, Glomar Shoal, located on the southwest corner of the sampling region, has anomalously low sand silt fractions. Active deposition of fine sediment classes on the mid shelf is restricted to localised areas (Brunskill et al. 2001), with typical weight fractions below 2% for silt and 0.5% for clay. However, conditions are less energetic on the outer shelf, where there is accumulation of silt and clay fractions (Jones, 1973; McLoughlin & Young, 1985). The transition from mid and outer shelf sediments occurs at the phi3 to phi4 size (figure 2.3.2).
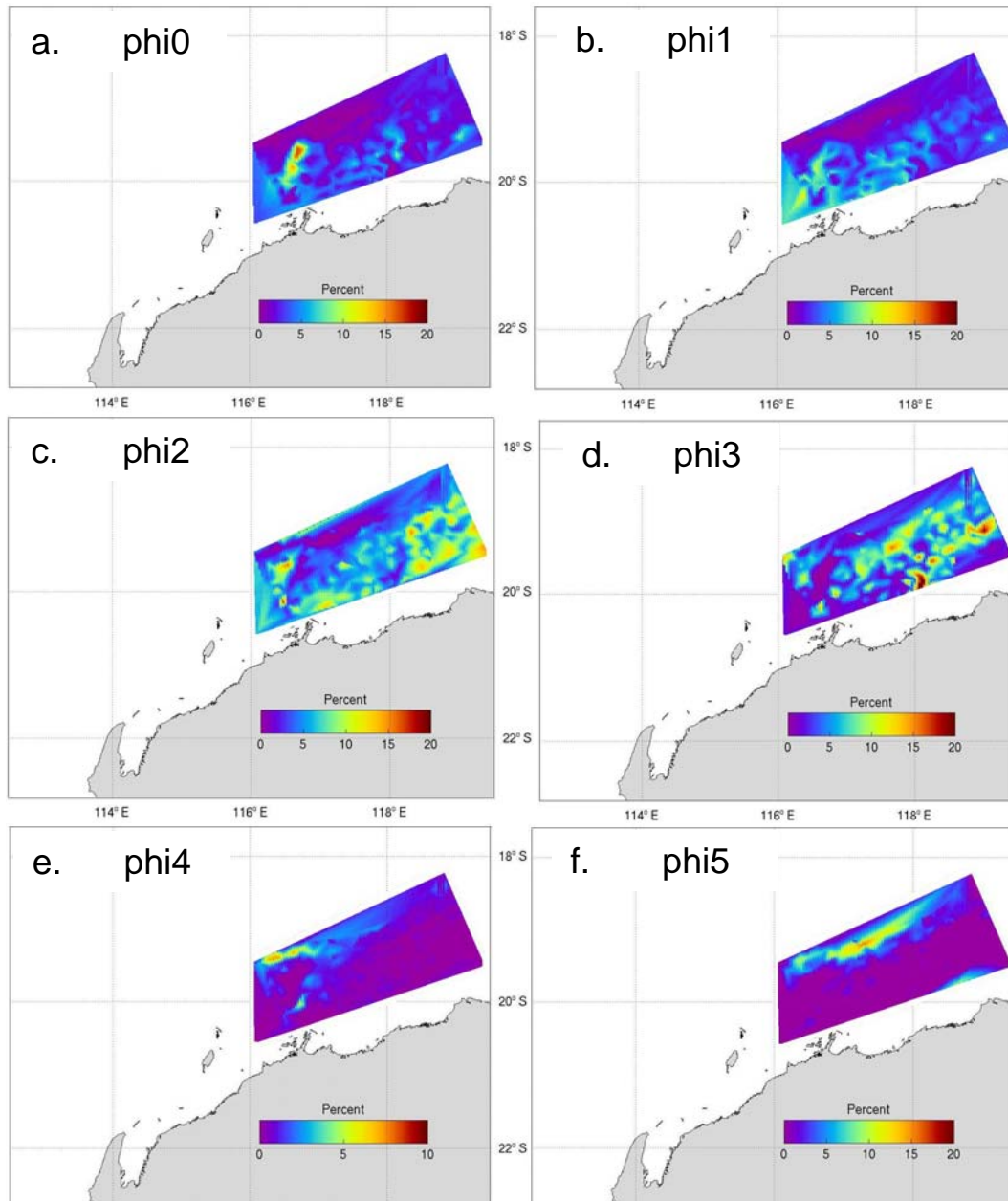
Figure 2.3.2: Distribution of sediment classes on part of the NWS from CSIRO data presented at 1 phi resolution.

The mean size spectrum of the shelf sediments calculated from the CSIRO data (figure 2.3.3) indicates that 2.5% of the sediment mass was composed of clay, 8% of silt, and 89.5% of gravel and sand fractions. Similar calculations based on samples collected only in areas shallower than 60 m depth give higher gravel and sand fractions (97.5%) and lower clay (0.5%) clay and silt (2%). The same trends are revealed by data collected a decade earlier by the Bureau of Mineral Resources (figures 2.3.1 and 2.3.4). For example, nearly all of the bottom sediments within the 15 to 40 m depth range consisted of gravel and sand in roughly equal proportions, while clay and silt represented less than 1% (figure 2.3.5). Gravel fractions decreased steadily offshore, allowing the sand fraction to increase out to the mid shelf, beyond which finer sediments became more significant.
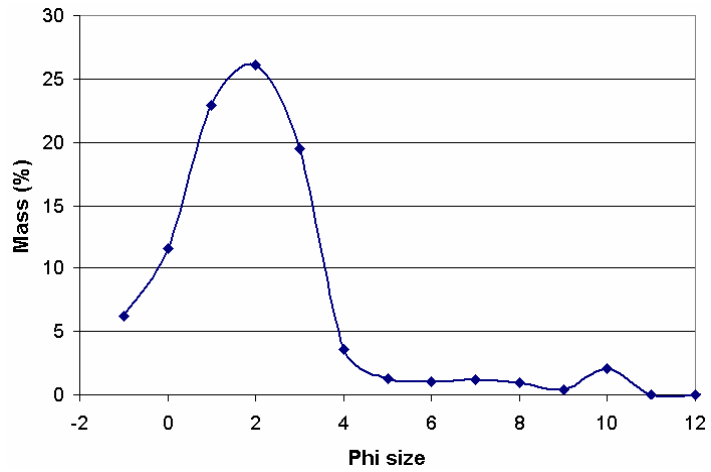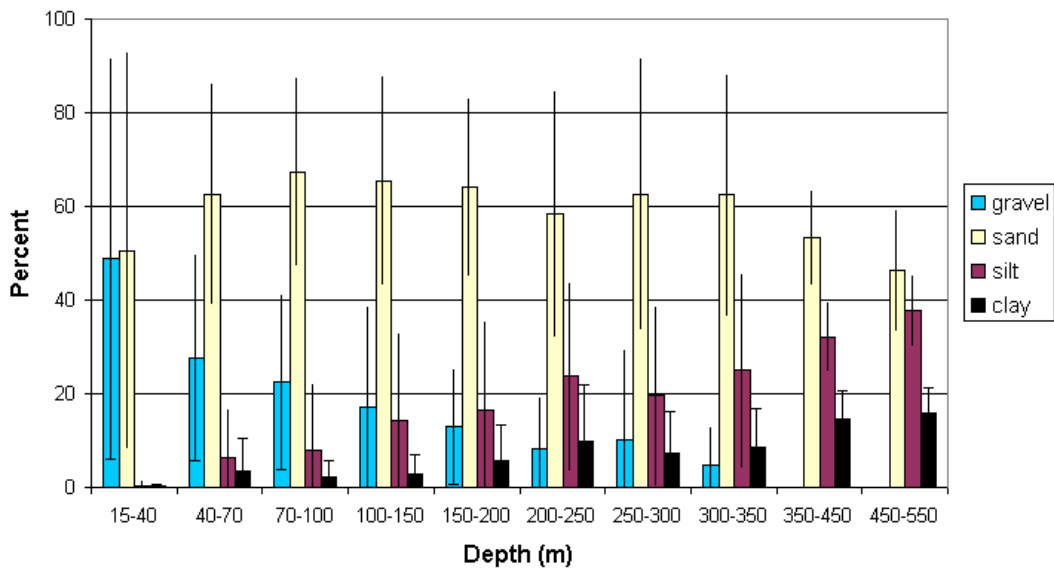
Fig 2.3.3: Sediment size spectrum of CSIRO data averaged across all the sampling sites shown in figure 2.3.1 (a) to a sediment depth of 10 cm.
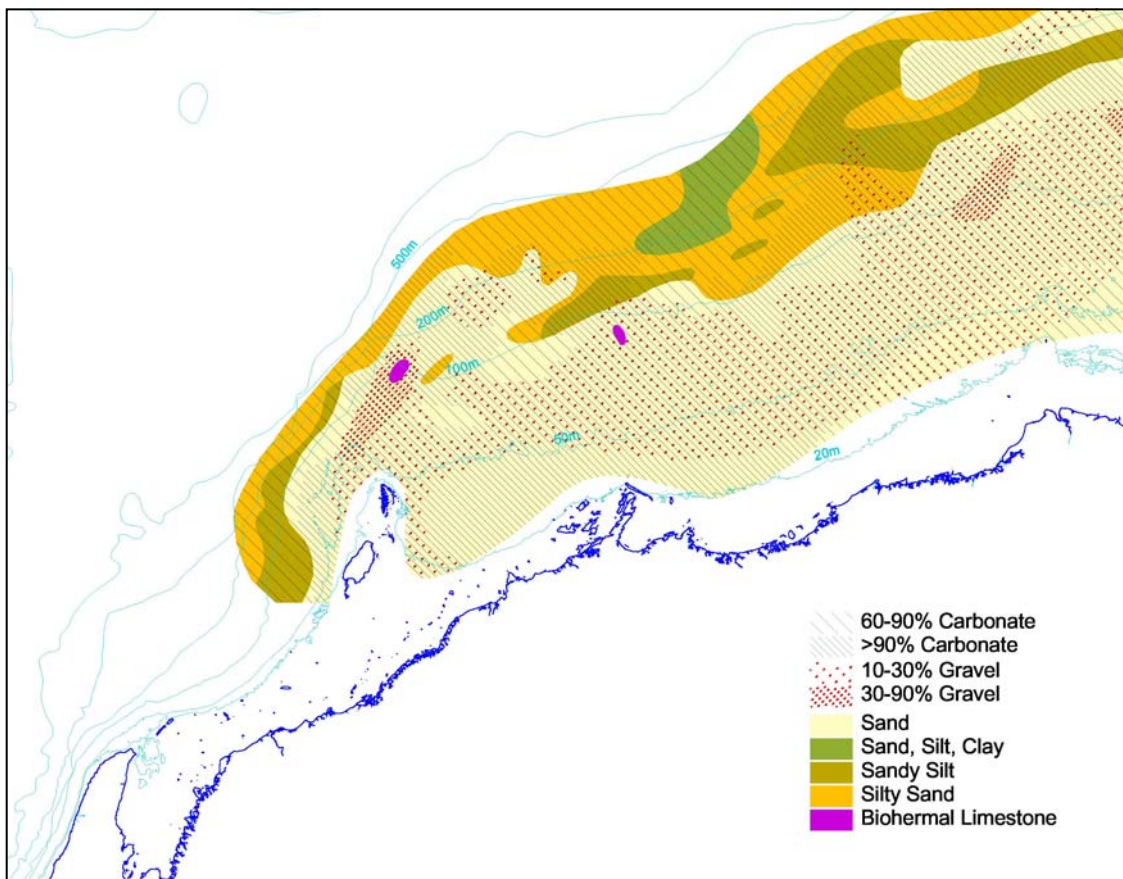

Figure 2.3.4: Sediment distribution from Bureau of Mineral Resources surveys of the North West Shelf conducted in 1967 and 1968 (Jones, 1973) provided by Geoscience Australia.

Figure 2.3.5: Sediment fraction as a function of water depth based on data from Bureau of Mineral Resources surveys of the North West Shelf conducted in 1967 and 1968 (Jones, 1973) provided by Geoscience Australia.

Little of the bottom sediment data discussed so far was derived from very shallow water (<10 m), which can exhibit quite different characteristics (Brunskill et al. 2001). For example, in the central region of Exmouth Gulf silt and clay fractions are around 20%, increasing to more than 40% on the salt flats (figure 2.3.6). These values are at least an order of magnitude higher than those found over the mid shelf.
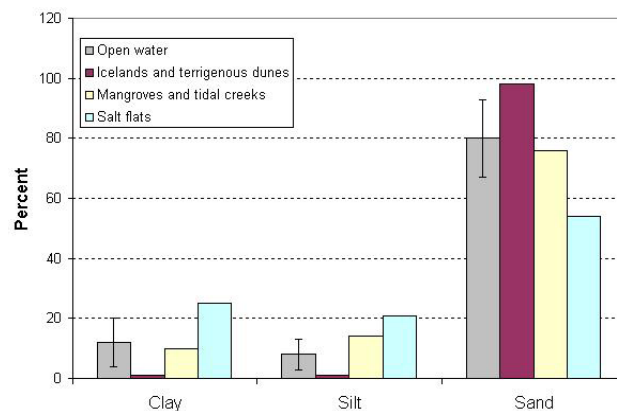
Figure 2.3.6: Sediment weight fractions in Exmouth Gulf habitats (Brunskill et al. 2001).

3.   MODEL DESCRIPTION

3.1   Model overview

In order to provide better understanding of the shelf sediment dynamics, a numerical model of the hydrodynamics and sediment transport was developed and implemented on the NWS. The coupled model was applied to simulate sediment fluxes in 1996, 1998, and 1999, and to investigate the impact of Tropical Cyclone Bobby on the redistribution of shelf-sediments in February 1995. The main objective of the simulations was to provide a quantitative assessment of the sediment fluxes on the shelf and evaluate their seasonal and annual variability. It also provided the basis for developing biogeochemical models of the NWS system as described by Herzfeld et al. (2006).

Water circulation was modelled using a three dimensional non-linear hydrodynamic model referred to as MECO (Model of Estuaries and Coastal Oceans; Herzfeld et al. 2006). This model has previously been applied to a range of estuarine and shelf systems, including the Gulf of Carpentaria (Condie et al. 1998), Port Philip Bay (Walker, 1999), and southeastern Australia (Bruce et al. 2001). Outputs from the circulation model typically included the three dimensional temperature, salinity, and current fields, as well as sea level, and bottom stress. Implementation of MECO for the NWS is described in more detail by Condie et al. (2006).

Sediment transport was modelled using a three dimensional sediment transport model fully coupled to MECO (Margvelashvili, 2003). This model calculated transport of particulate, dissolved, and sediment-bound tracers in the water column and in the sediment bed, while neglecting any bed load contribution. The complete model consisted of several integrated modules dealing with sediment transport, dissolved and sediment-bound tracers, and the bottom-boundary layer.

The sediment transport module solved an advection-diffusion equation for the mass conservation of suspended and bottom sediments, taking into account bottom exchanges by resuspension and deposition. Turbulent mixing in the water column and horizontal advection were driven using inputs from the hydrodynamic model. Any feedback between suspended sediment and the density stratification was neglected. Displacement of particles in the sediment bed was included through bioturbation, swelling and consolidation. Bioturbation was represented by local diffusion. Cohesive sediments were either eroded or deposited depending on bottom shear stresses and critical shear stresses. The concept of equilibrium sediment distribution was used to parameterise the erosion and deposition of non-cohesive sediment. To calculate erosion on a mixed multi-grain sediment bed, the model utilised the concept of an active sediment layer, whereby sediment particles were available for resuspension from the top sediment layer during each computational time step.

Bottom friction under combined wave-currents was calculated using the Grant and Madsen (1994) model. On a cohesive sediment bed, constant physical roughness associated with biogenic bed-forms was specified. On a non-cohesive sediment bed the total physical roughness was assumed to be composed of skin friction at the bed and form drag over ripples. The bed forms were specified as model input parameters.

The model governing equations were formulated in a time-varying sediment-thickness-adapted coordinate frame. The numerical solution of the transport equation utilised an implicit finite-difference scheme for advective and diffusive terms. The sediment settling term was approximated using an upwind finite-difference scheme, while horizontal advection was calculated using the Van Leer numerical scheme. The governing equations were transformed to a three-diagonal system of algebraic equations, which was then solved using Thompson's method. The main model parameters are summarised in table 3.2.1 and fully documented in the model documentation (Margvelashvili, 2003).

Numerical solutions were computed on both fine (5 by 5 km) and coarse (20 by 10 km) resolution grids, both covering the same domain extending from the coast to beyond the shelf break over the Pilbara coastline from Exmouth Gulf to Port Hedland. The vertical resolution was the same for both grids, expanding from three metres near the surface to a maximum of 21 m at depths below 200 m. The maximum depth offshore was limited to 300 m. This had only a minor impact on shelf processes, but substantially improved computational efficiency. The fine resolution grid was identical to the "Pilbara model" grid used by Condie et al. (2006). The horizontal resolution in the sediment bed was the same as that in water column, with five layers in the vertical. The initial thickness of the sediment bed was set at 0.5 m, after which each layer was allowed to change with time.

3.2 Boundary and initial conditions.

The lateral boundary conditions required to force the hydrodynamic model were temperature, salinity, and sea level. These fields were provided by interpolating outputs from a larger scale regional model referred to as the "Northwest model" (also based on MECO), which in turn was nested within a global model (based on the Australian Community Ocean Model; Schiller et al. 2000). Details of the nesting strategy are described by Condie et al. (2006). Lateral boundary conditions for suspended sediment concentrations were also required wherever flow was directed into the model domain. In the absence of better information, it was assumed that concentrations were largely controlled by local deposition and suspension, so that boundary values could be adequately approximated by mean values calculated over a boundary sub-region.

The model was forced at the surface by wind fields taken from the NCEP-NCAR 40-year re-analysis data set (Kalnay et al. 1996). However, tropical cyclones could be represented by higher resolution winds generated by the Holland (1980) model nested into the broader scale patterns provided by the NCEP-NCAR product. Surface wave characteristics on the NWS were modelled using a simple empirical formulation (U.S. Army Coastal Engineering Research Center, 1984) as described by Condie and Andrewartha (2002). This model assumed a fully developed sea state and required only the wind speed, fetch, and water depth as inputs. The near-bottom wave orbital velocity, direction, and frequency calculated by the wave model were used by the bottom boundary layer module to calculate bottom shear stresses (figure 3.2.1).

Table 3.2.1: List of model parameters (as described fully in the model documentation, Margvelashvili, 2003) and values used in the NWS model.

Parameter	Description	Dimension	Cited values	Model values
ρ^w	Water density	kg (m^{-3} water)	1025	1025
ρ_i^s	Sediment density	kg (m^{-3} solid)	-	2650
v_i^s	Vertical diffusion coefficient for solid particles in sediment bed	m^2 s^{-1}	$10^{-11} - 10^{-9}$	10^{-11}
a	Empirical constant in the formula for equilibrium concentration of non-cohesive sediments (model documentation, eq. 3.7)	none	$10^{-5} - 2 \times 10^{-3}$	2×10^{-3}
z_r	Reference height in the formula for equilibrium concentration of non-cohesive sediments (model documentation, eq. 3.7)	m	$3 \sim 7$ (grain diameters)	1×10^{-3}
M	Empirical constant in the formula for cohesive sediment resuspension (model documentation, eq. 4.8)	kg m^{-2} s^{-1}	$1.7 \times 10^{-5} - 4.4 \times 10^{-3}$	$0.002\,\tau_{ce}$
τ_{ce}	Critical shear stresses of cohesive sediment erosion	N m^{-2}	$0.05 - 5$	0.2
τ_{cd}	Critical shear stresses of cohesive sediment deposition	N m^{-2}	$0.2 - 10$	∞
z_o	Bottom grain roughness parameter	m	$2 \times 10^{-3} - 10^{-5}$	2×10^{-4}
h_a	Thickness of an active sediment layer	m	$0 - 0.007$	0.005, 0.0025
η	Ripples height	m	$0 - 1$	0.015, 0.03
λ	Ripples length	m	$0 - 10$	0.4
v_o^s	Diffusion coefficient for mixing of the solid particles across "sediment – water" interface	m^2 s^{-1}	-	10^{-11}
p	K-sigma grid weighting constant (model documentation, eq. 7.20)	none	-	10^{-4}
k	von Karman's constant	none	0.42	0.42
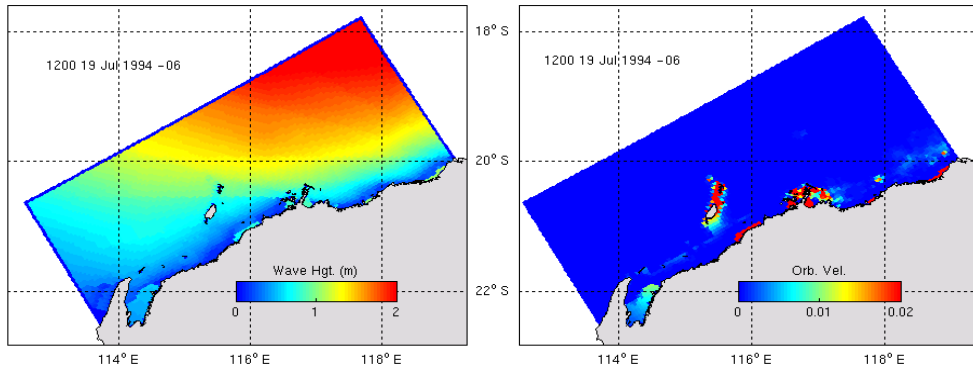
Figure 3.2.1: Example of significant wave-height (left) and bottom orbital velocity (right) for July 1994 from the simple wave model (Condie & Andrewartha, 2002).

Initial conditions for the hydrodynamic model were interpolated from the Northwest model ensuring consistency with the boundary conditions. Suspended sediment concentrations were initially set to zero and allowed to evolve through resuspension and deposition. However, this evolution was sensitive to the availability of each sediment fraction (figure 3.2.2), suggesting that accurate initialisation of the bottom sediments was critical. Hence, they were initiated using the size spectrum derived from CSIRO data (figure 2.3.3) assuming that each sediment fraction was evenly distributed over the whole modelling domain. Eight sediment sizes were modelled with one phi resolution, assuming a constant settling velocity for each taken from the Coastal Engineering Manual (1999) (table 3.2.2). Because significant errors can arise when modeling transport of coarse sediments on a z-coordinate numerical grid, the horizontal advection of only fine sediment fractions was calculated. A vertical one dimensional calculation was applied to the coarse sediments (phi1 and phi2 fractions) allowing local resuspension and deposition, but no horizontal exchange between grid cells.
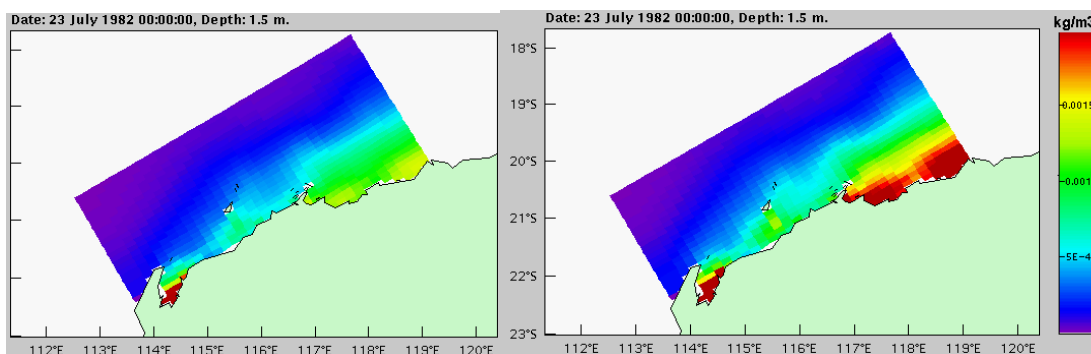
Figure 3.2.2: Modelled surface concentrations of fine sediment modelled using initial fine bottom sediment concentrations of 1 kg m^{-3} (left) and 2 kg m^{-3} (right).

Table 3.2.2: Sediment settling velocities (W) specified according to the Coastal Engineering Manual (1999).

| Fraction	Coarse sand	Medium sand	Fine sand	Very fine sand	Coarse silt	Medium silt	Fine silt	Unfloc. clay
Size (phi)	1	2	3	4	5	6	7	
W (m/s)	0.074	0.0323	0.0111	0.0032	0.00081	0.0002	$5.79e^{-5}$	$1.0e^{-5}$

4.   MODEL RESULTS

4.1   Preliminary model runs

### 4.1.1   Sensitivity to boundary sediment concentrations

The boundary condition used for suspended sediments essentially assumed that conditions upstream of the boundary were similar to those a short distance downstream. This condition was adopted because more reliable information was not available. Model runs were therefore undertaken to evaluate the role of boundary inputs on the distribution of tracers within the modelling domain. Three types of conservative tracers (zero settling velocity) were specified at the northeastern, southwestern and offshore lateral boundaries (one tracer per boundary). Initial concentrations of all tracers inside the domain were set to zero. After running the coarse resolution model over a few months most of the water initially in the model domain had been replaced by water from the lateral boundaries (figure 4.1.1). Water on the shelf was derived mostly from the northeast during this period, with a substantial contribution to the waters southwest of Dampier from the offshore boundary. The southwesterly boundary only became significant at depths greater than 50 m. However, these patterns were highly seasonal, with the influence of the northeasterly boundary peaking with the Leeuwin Current in Autumn and then declining to a minimum in Spring when offshore influences were more dominant (figure 4.1.2).

4.1.2   Sensitivity to initial seabed concentrations

The potential for mid to outer shelf regions to deliver fine sediments inshore was tested using model runs with a highly simplified distribution of bottom sediment. Concentrations were set to zero shoreward of either the 50 m or 150 m isobath (figure 4.1.3), so that the only sediments arriving inshore were those resuspended in deeper water. Results suggest that there were no significant landward fluxes of fine sediments offshore of 150 m. However, those eroded between 50 m and 150 m northeast of Dampier contributed significantly to the inshore turbidity maximum. The size spectrum from this region (figures 2.3.1 (a) and 2.3.3) was therefore used to initialise the bottom sediment concentration in all subsequent model runs.
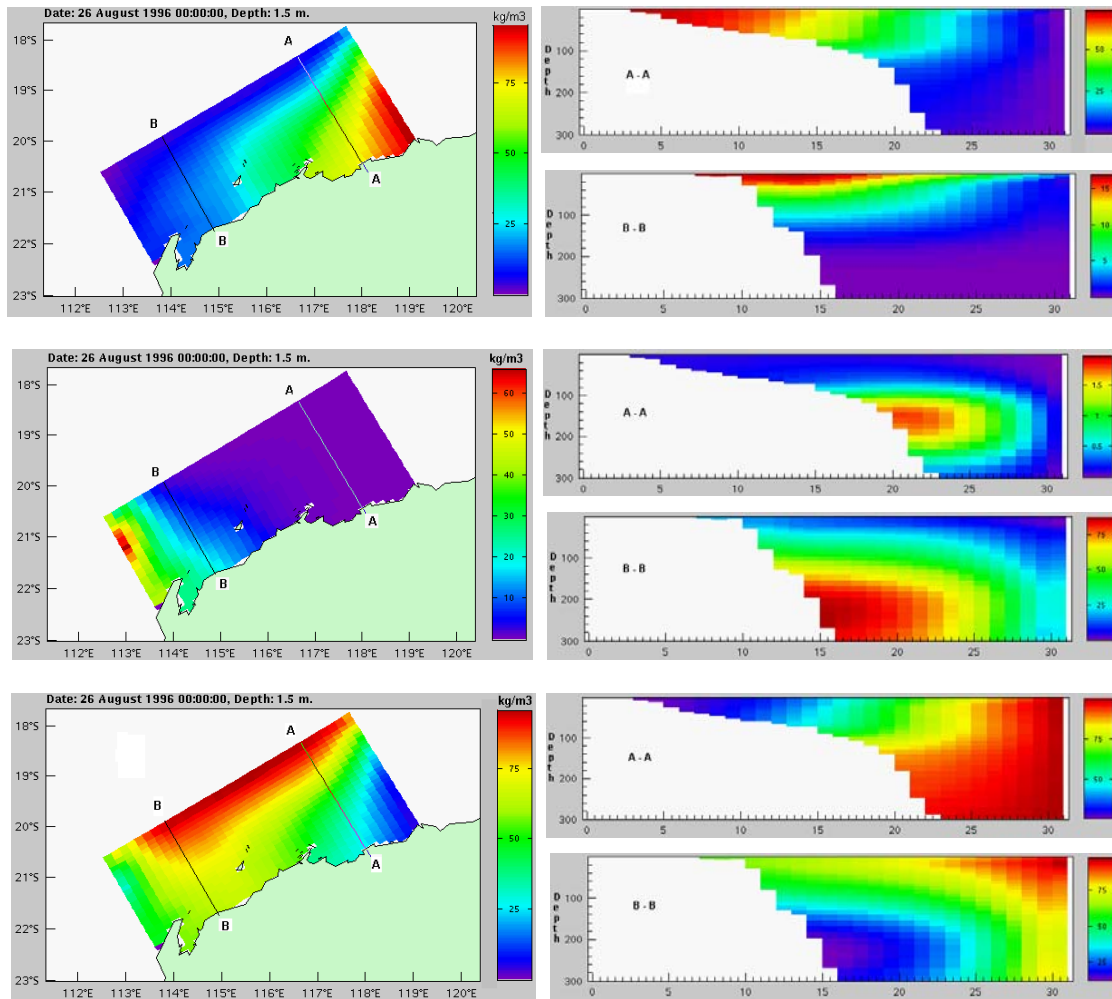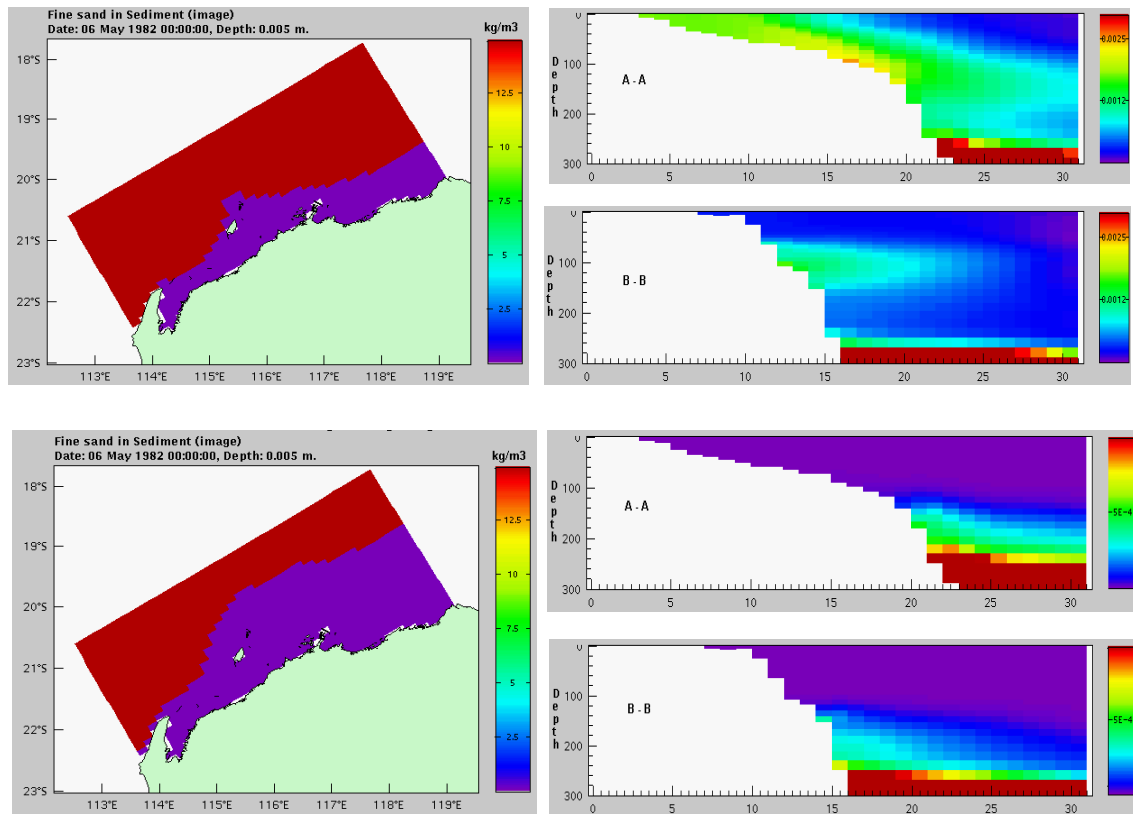
Figure 4.1.1: Surface concentration (left) and cross-shore vertical sections (right) of tracers released at the northeastern boundary (top), southwestern boundary (centre), and offshore boundary (bottom). The concentration of a particular tracer at a given point represents the percentage of water from the release boundary.
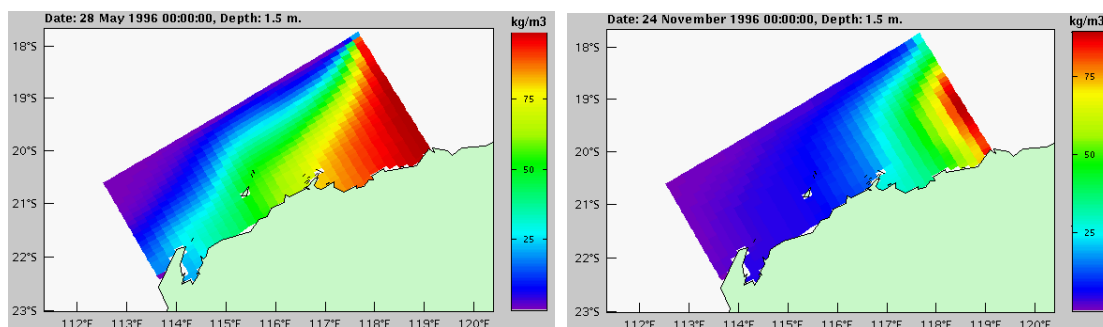
Figure 4.1.2: Surface concentration of the tracers released at northeastern boundary through Autumn (left) and Spring (right).

Figure 4.1.3: Fine bottom sediment concentration (left) and cross-shore vertical sections of suspended sediment concentration (right) from scenarios with zero initial bottom concentration inshore of the 50 m isobath (upper) and 150 m isobath (lower). The locations of the sections (A-A and B-B) are shown in figure 4.1.1.

4.2   Annual simulations

This section describes the results from a series of year long simulations run for the years 1996, 1998, and 1999.

4.2.1   Bottom stress distributions

Resuspension in the model varied strongly over the course of the spring neap tidal cycle in response to changing bottom stress. These results are presented in terms of model estimates of the bottom shear velocity (equal to the square root of bottom stress divided by water density). Time series of bottom shear velocity at five sites on the NWS (figure 2.1.1) indicate that the threshold for resuspension was frequently exceeded at the depths shallower than 60 m, but rarely at 150 m depth (figure 4.2.1). At the Exmouth Gulf site this threshold was exceeded at some point during nearly every flood-ebb cycle, while at Dampier and Port Hedland it typically only occurred within the week either side of spring tide. Resuspension was more closely confined to spring tide at 60 m, while at 150 m it occurred only very rarely during 1996 and 1999 (not shown) and not at all in 1998 (figure 4.2.1).

The spatial distribution of shear velocity across the NWS can be illustrated by monthly mean fields (figure 4.2.2). Maximum shear velocities occurred in Exmouth Gulf, around Barrow and the Monte Bello Islands, and over the broad inner shelf region to the east. General patterns in monthly shear stresses did not change significantly between seasons or years, again reflecting the dominant role of the spring neap cycle.
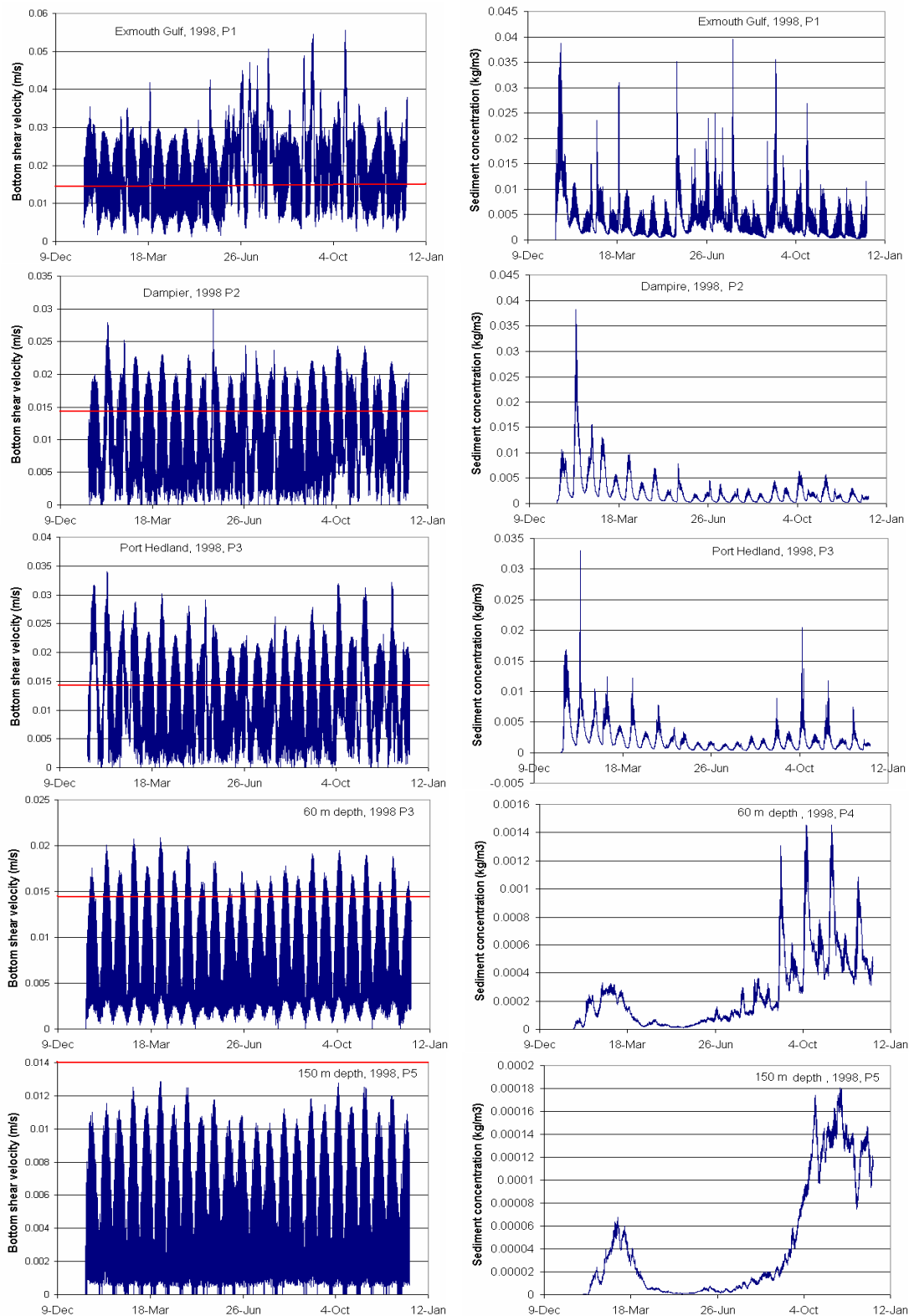
Figure 4.2.1: Calculated bottom shear velocities (left) and surface suspended sediment concentration (right) during 1998 at sites P1 in Exmouth Gulf, P2 near Dampier, P3 near Port Hedland (all at 10 m depth), and P3 (60 m) and P5 (150 m) offshore of Port Hedland (all sites are shown in figure 2.1.1). The red lines indicate the approximate bottom shear velocity threshold for resuspension for fine sediments (0.014 m s^{-1} or 0.2 N m^{-2}).
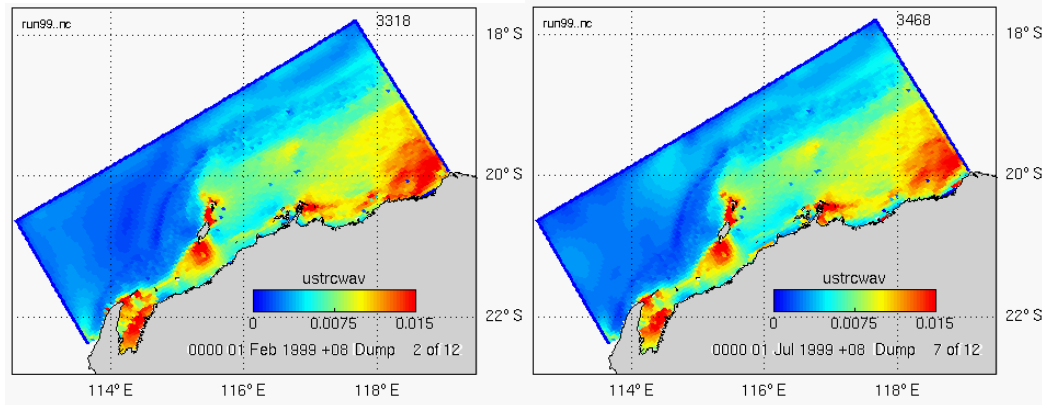
Figure 4.2.2: Monthly averaged bottom shear velocity (m s^{-1}) for February 1998 (left) and July 1998 (right).

4.2.2 Suspended sediment distributions

Suspended sediment concentrations varied significantly, particularly across the spring neap cycle. However, the spatial pattern was always characterised by elevated concentrations along the inner shelf (figure 4.2.3), which contracted towards the coast with increasing grain size (figure 4.2.4). This result is qualitatively consistent with the turbidity patterns derived from satellite ocean-colour data (figure 2.2.1). Average surface values in shallow waters (<30 m) from Exmouth Gulf to Barrow Island range from 1×10^{-3} to 2.5×10^{-3} kg m^{-3} (figure 4.2.3), which is consistent with the available observations (figures 2.2.3 and 2.2.4).

Time series indicate that suspended concentrations over the inner shelf typically climbed from neap-tide lows of less than 10^{-3} kg m^{-3} to spring tide highs of 10^{-2} kg m^{-3}, with occasional spikes approaching 4×10^{-2} kg m^{-3} (figure 4.2.1). Concentration peaks generally corresponded to peaks in bottom shear velocity at the same site, although larger shears did not necessarily produce larger concentration spikes.
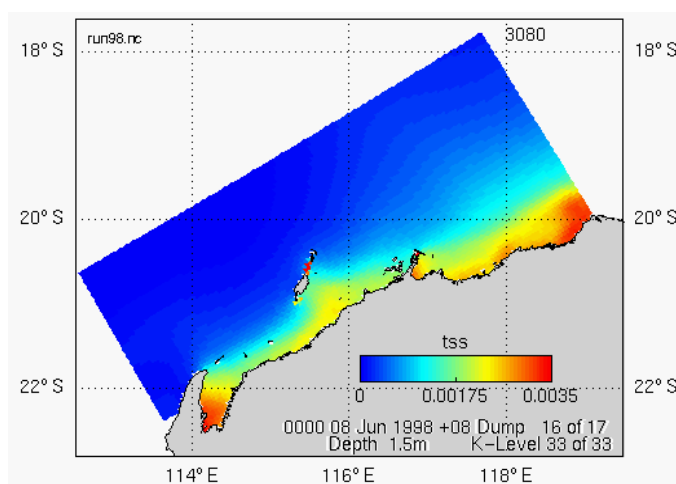
Figure 4.2.3: Modelled surface concentrations (kg m^{-3}) of total suspended sediments in June 1998 at approximately the midpoint between neap and spring tide.
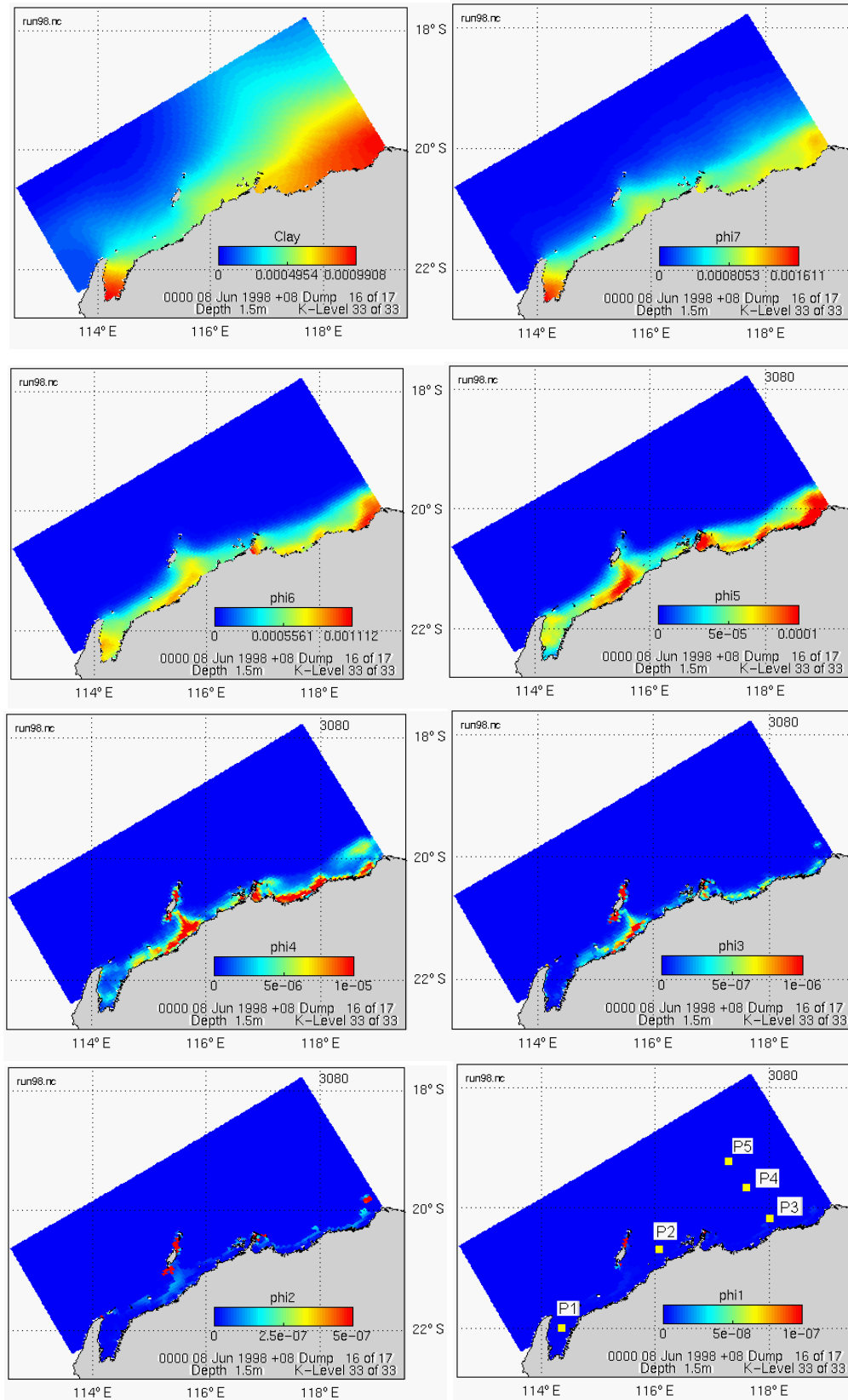
Figure 4.2.4: Modelled surface concentrations (kg m^{-3}) of sediments fractions for each size class (in order of increasing size) at approximately the midpoint between neap and spring tide. Locations of sites used for time series analysis are also indicated on the phi1 map (bottom right).

Over the mid and outer shelf concentrations rarely exceeded 10^{-3} kg m^{-3} and were often much smaller (figure 4.2.1). They were also less dependent on the spring neap cycle, but could be significantly influenced by the direction of the prevailing (sub-tidal) circulation. In particular, concentrations at P3 and P5 tended to be high when the circulation was northeastward (September to February) and low when it was southwestward (April to August). In the latter circumstances, model concentrations at these two sites may have been significantly influenced by the northeast boundary conditions. Unfortunately there are no observations in this area for comparison.

Settling fluxes could be inferred from model sediment concentrations (figure 4.2.4) and settling velocities (table 3.2.2). Peak values over the inner shelf approached 50 g m^{-2} day^{-1}, but like suspended sediment levels diminished rapidly over the mid and outer shelf. Model values over the outer shelf and slope where in the range 102 to103 mg m^{-2} day^{-1}, which is consistent with sediment trap observations (322 to 616 mg m^{-2} day^{-1}) reported recently by Burns et al. (2003).

4.2.3   Bottom sediment distributions

Observations indicate that fine sediments are resuspended over the energetic inner and mid shelf environments and deposited further offshore. Available data indicates that the transition between sediments winnowed from the shelf and sediments remaining on the shelf occurs at approximately the phi3 to phi4 size class (figure 2.3.2). This pattern was reproduced by the model with silt and clay fractions resuspended and winnowed from the shelf then deposited offshore, while sand fractions were mainly redistributed within the shelf region (figure 4.2.5). Concentrations of fine sediments immediately beyond the shelf break were lower than those in more distant offshore regions (clay and phi7 in figure 4.2.5). This is explained by intensive deposition and accumulation of coarser sediment fractions beyond the shelf break that reduced the concentration of the finer sediments (phi6 to phi4 in figure 4.2.5). These trends were evident in all three simulated years, as illustrated for example by the fine sediment fractions in 1996 and 1999 (figure 4.2.6).

4.2.4   Sediment fluxes

The NWS narrows towards the southwest and almost vanishes at the North West Cape (figure 2.1.1). One consequence is that alongshore fluxes directed towards the southwest eventually flow off the shelf. Here we define an offshore flux as one crossing the 150 m isobath, while alongshore fluxes are evaluated at the northeast model boundary over depths shallower than 150 m.

Offshore fluxes consisted mainly of fine sediment fractions being transported onto the continental slope, with some enhancement in autumn and winter under the influence of southeasterly trade winds (figure 4.2.7). Coarser sediments were moved offshore more periodically in events usually aligned with spring tides. Alongshore fluxes consisted mainly of coarse sediments directed to the southwest and were again aligned with the spring tide period (figure 4.2.8).

The year 1998 used in the above examples (figures 4.2.7 and 4.2.8) was notable for the absence of extreme weather events. However, tropical cyclones are common on the NWS and had a dramatic impact on sediment fluxes in other years (figures 4.2.9 and 4.2.10). For example, peak fluxes of total suspended sediment around 20 March 1999

coincide in time with the arrival of Tropical Cyclone Vance, while those in April 1996 can be attributed to Tropical Cyclone Olivia, which crossed the Pilbara coast on 10 April 1996. These peaks were at least an order of magnitude greater than those produced during springtides, and may have been much larger if the cyclone winds had been better resolved by the NCEP-NCAR fields (see section 4.3).
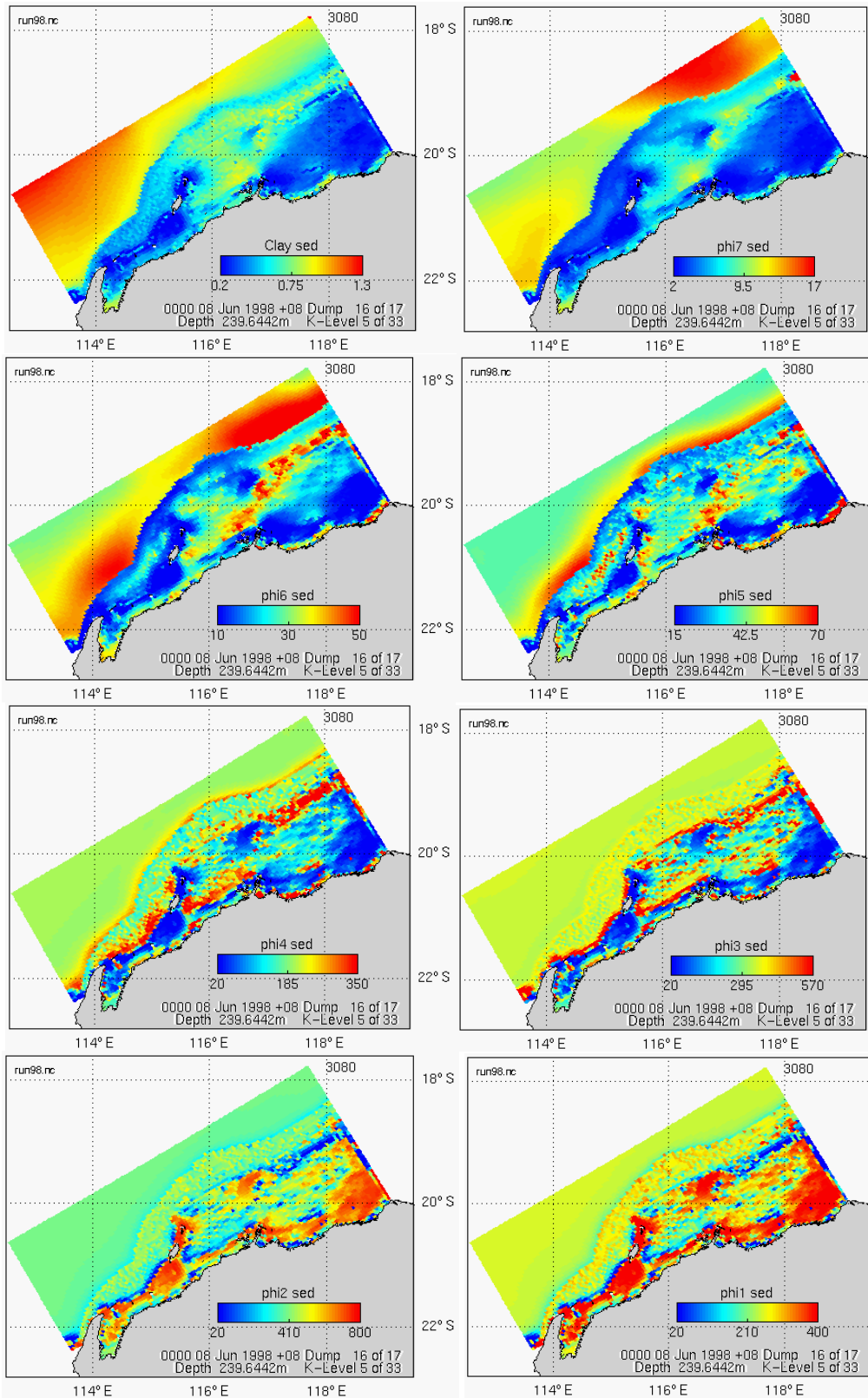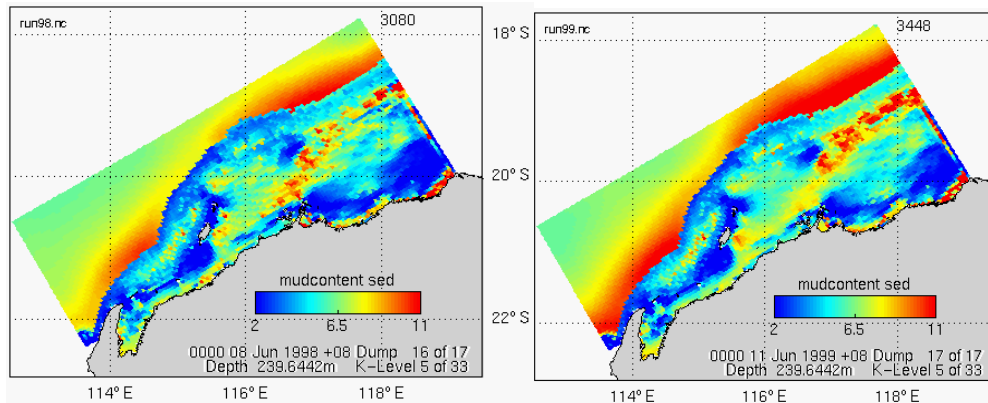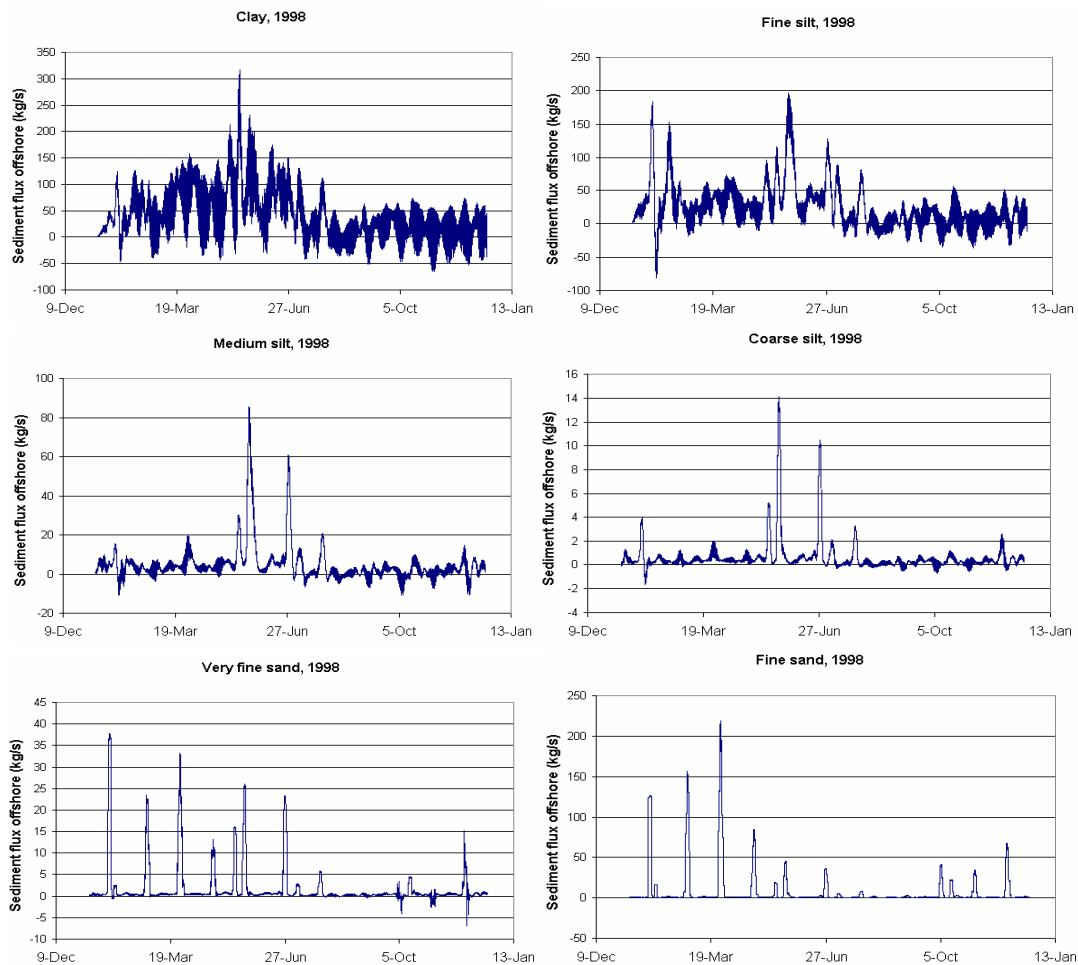
Figure 4.2.5: Modelled distribution of the bottom sediment classes (kg m^{-3}) in June 1998.
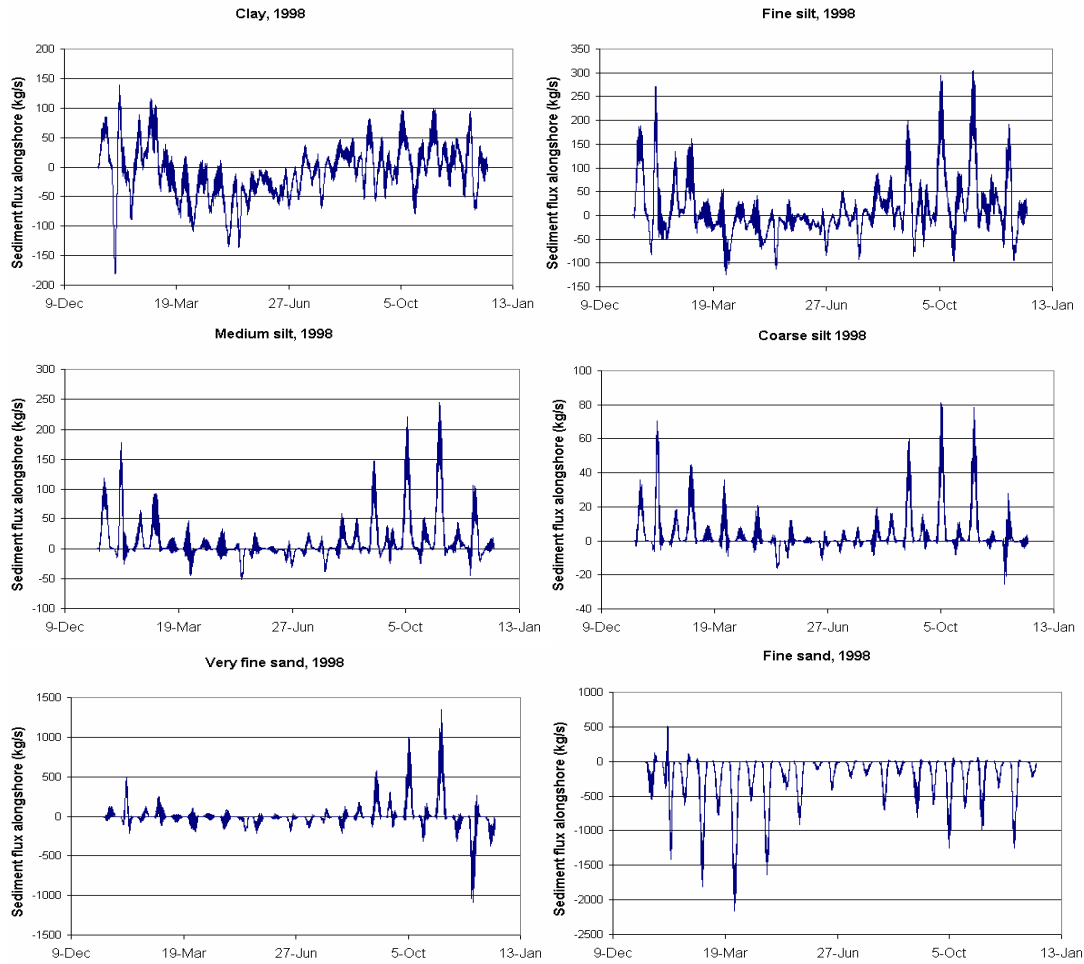
Figure 4.2.6: Simulated distribution of fine bottom sediments (kg m^{-3} of clay plus the three silt fractions) in June 1996 (left) and June 1999 (right).
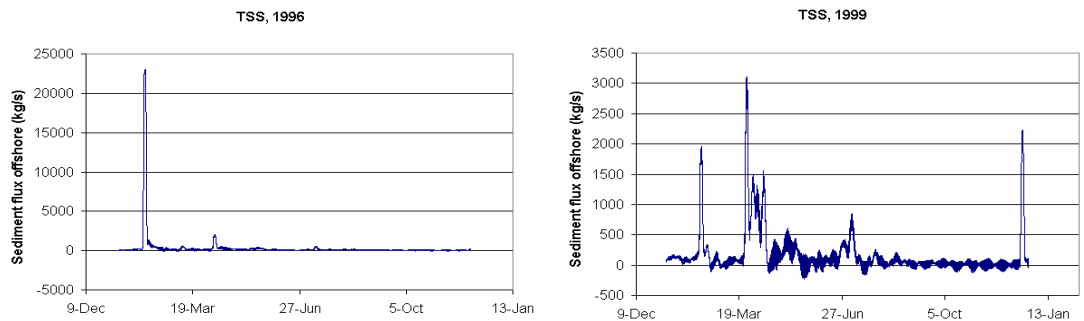

Figure 4.2.7: Modelled offshore fluxes of various sediment classes during 1998. Fluxes were positive when directed offshore. A three day filter was applied to remove high frequency tidal oscillations.

Figure 4.2.8: Modelled fluxes of various sediment classes at the northeast model boundary during 1998. Fluxes were positive when directed to the northeast (i.e. out of the model domain). A three day filter was applied to remove high frequency tidal oscillations.

Figure 4.2.9: Modelled total offshore sediment flux during 1996 (left) and 1999 (right). Fluxes were positive when directed offshore. A three day filter was applied to remove high frequency tidal oscillations.
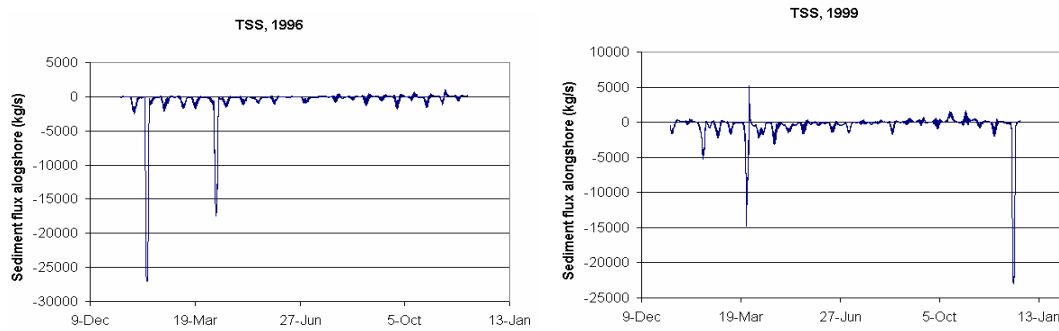
Figure 4.2.10: Modelled total alongshore sediment flux during 1996 (left) and 1999 (right). Fluxes were positive when directed to the northeast. A three day filter was applied to remove high frequency tidal oscillations.

Annual mean total sediment fluxes are summarised in table 4.2.1. There was a persistent discharge of sediments at the offshore boundary, while alongshore fluxes at the northeast boundary delivered sediments into the modelling domain. The net balance of the alongshore and offshore fluxes was negative and therefore represented sediment accumulation on the shelf. The accumulation contained predominantly sand fractions. This sand was mobile in shallow regions producing strong fluxes at the northeast boundary (figure 4.2.8), while on the outer shelf it was less frequently resuspended and contributed little to the offshore flux.

In contrast to the sand fractions, mean offshore fluxes of fine sediments (silt and clay) were greater than the corresponding alongshore fluxes (table 4.2.2.). Those at the offshore boundary were directed into deeper water. This direction is consistent with fine sediment fluxes from the two dimensional model of Ribbe and Holloway (2001), although without winds or regional circulation in their model the magnitude of the flux was negligible in waters deeper than 120 m. The alongshore fluxes imported fine sediments from the northeast in 1996 and 1999 and exported them to the northeast in 1998. The balance of the alongshore and offshore fluxes corresponded to a net offshore export of fine sediments in all three years.

Table 4.2.1: Annual mean total sediment fluxes on the NWS.

Year	Offshore flux (kg s^{-1})	Alongshore flux (kg s^{-1})	Balance (kg s^{-1})
1996	331	-617	-286
1998	81	-156	-75
1999	178	-509	-331

Table 4.2.2: Annual mean fine sediment fluxes (silt and clay fractions) on the NWS.

Year	Offshore flux (kg s^{-1})	Alongshore flux (kg s^{-1})	Balance (kg s^{-1})
1996	154	-68	86
1998	72	22	94
1999	134	-21	113

The annual sediment supply from rivers on the NWS is relatively modest averaging approximately 27 kg s^{-1} (figure 2.2.2). However, the model results suggest that this may be comparable to the alongshore flux and a significant fraction (~30%) of the net export of fine sediments (table 4.2.2). To further evaluate the fate of river sediments, idealised model runs were undertaken in which mean annual loads from major Pilbara rivers were represented by point sources of fine sediment (figure 2.2.2). The highly seasonal nature of the river flow was approximated by allocating the annual sediment load to the first three months of the calendar year. Initial concentrations of sediments in both the water column and sediment bed were set to zero. As the grain size distribution for river sediments was not known, they were represented by medium and fine silt fractions. The model results indicated that river sediments were initially deposited around the river mouths and on the neighbouring inner shelf with a bias to the northeast (figure 4.2.10). However, they were subsequently resuspended over autumn and transported across the shelf break under the influence of the southeasterly trade winds.
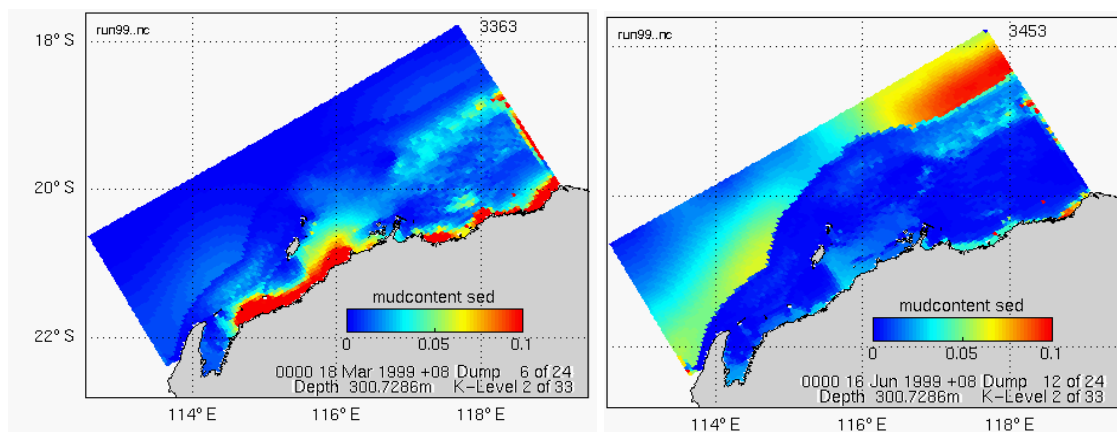

Figure 4.2.10: Calculated redistribution of river sediments (kg m^{-3}) from March (left) to June (right) assuming river inputs ceased at the end of March.

The overall picture of sediment transport suggested by the model is of sandy sediments moving southwestward, with about half eventually being exported offshore and the remainder accumulating on the shelf. Finer sediments also arrive from the northeast, with similar amounts supplied by seasonal river inputs. However, larger quantities are exported offshore leaving a net loss of fine sediments from the shelf. While the implied rates of annual sediment accumulation or loss are feasible, the errors in such estimates are likely to be significant.

4.3   Cyclone simulations

During the summer period tropical cyclones can generate major fluctuations in waves and current patterns on the NWS (Condie & Andrewartha, 2002; Condie et al. 2006). It has already been demonstrated that even when cyclone winds were severely under-resolved in the model (NCEP-NCAR), the impacts on sediment transports were substantial (figures 4.2.9 and 4.2.10). In order to more realistically evaluate these impacts, wind and pressure fields from a tropical cyclone model have been used to drive the sediment transport model. The case study presented below simulated the ocean and seabed response to Tropical Cyclone Bobby, which entered the modelling domain on 23 February and crossed the Pilbara coast on 25 February (figure 4.3.1).
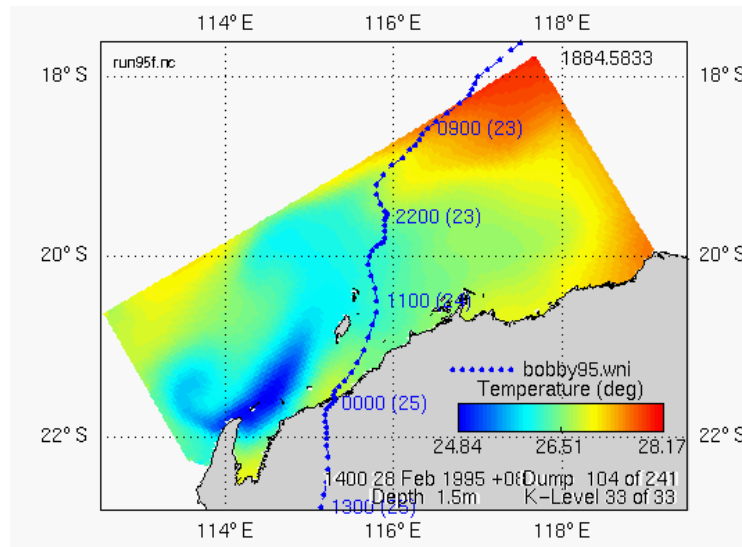
Figure 4.3.1: Cyclone track overlain on modelled sea surface temperature (°C). The track is labelled with the time (and date) corresponding to the eye of the cyclone, while the sea surface temperature corresponds to 1400 on 28 February.

The model was run over the period from 20 February to 1 March 1999. The local wind and pressure fields around the cyclone were simulated using the Holland (1980) model nested within the larger-scale NCEP-NCAR winds as described by Condie et al. (2004). Because the wave model assumption of a fully developed sea state was strongly violated under cyclonic conditions, wave fields based on the original NCEP-NCAR winds were retained for these model runs. As in other model runs, the initial concentration of suspended sediment was set to zero, while bottom concentrations followed the size spectrum in figure 2.3.3 assuming that each sediment fraction was evenly distributed over the modelling domain.

Bottom shear velocities were strongly enhanced in shallow water by the presence of Tropical Cyclone Bobby. The threshold for resuspension (0.014 m s^{-1}) was exceeded at coastal and offshore sites out to at least 150 m depth, with peak values reaching five times this level near Port Hedland (figure 4.3.2). The model predicted maximum shear stresses between Barrow and the Monte Bello Islands, and on the inner shelf northeast from the Dampier Archipelago (figure 4.3.3). Additional model runs conducted without the inclusion of wind-waves clearly demonstrate their substantial enhancement of the bottom shear velocity field on the inner shelf under cyclone conditions (figures 4.3.3 (b) and 4.3.3 (d)).

Surface concentrations of suspended sediments increased more than two orders of magnitude during the cyclone (figure 4.3.2). The maximum surface turbidity occurred along the coastline and around the Barrow and Monte Bello Islands (4.3.4). Inclusion of wind-waves in the model had a very substantial impact on suspended concentrations, typically increasing them by an order of magnitude (figures 4.3.4 (b) and 4.3.4 (d)).

The cyclone changed the thermohaline structure, circulation pattern, and suspended sediment distribution over the shelf, with some features persisting for up to two weeks after the event. Intensive upwelling occurred around North West Cape, where the converging flow produced a cold-core cyclonic (clockwise) eddy below the thermocline (figure 4.3.5). Near the surface the cold-water anomaly was advected along the edge of the shelf to the northeast, until leaving the shelf off Barrow Island and breaking up into a dipolar structure over deeper water. This flow carried sediments well offshore, where they settled out of the surface layers over the following few days (figure 4.3.6). The warm core of the anti-cyclonic side of the dipole penetrated down to 150 m (figure 4.3.5) and entrained sediments into a concentrated cloud ($\sim$0.03 kg m^{-3}) located northwest of Barrow Island (figure 4.3.6). Here the sediments settled onto the seabed as localised depositions up to 0.4 m thick (figure 4.3.7).
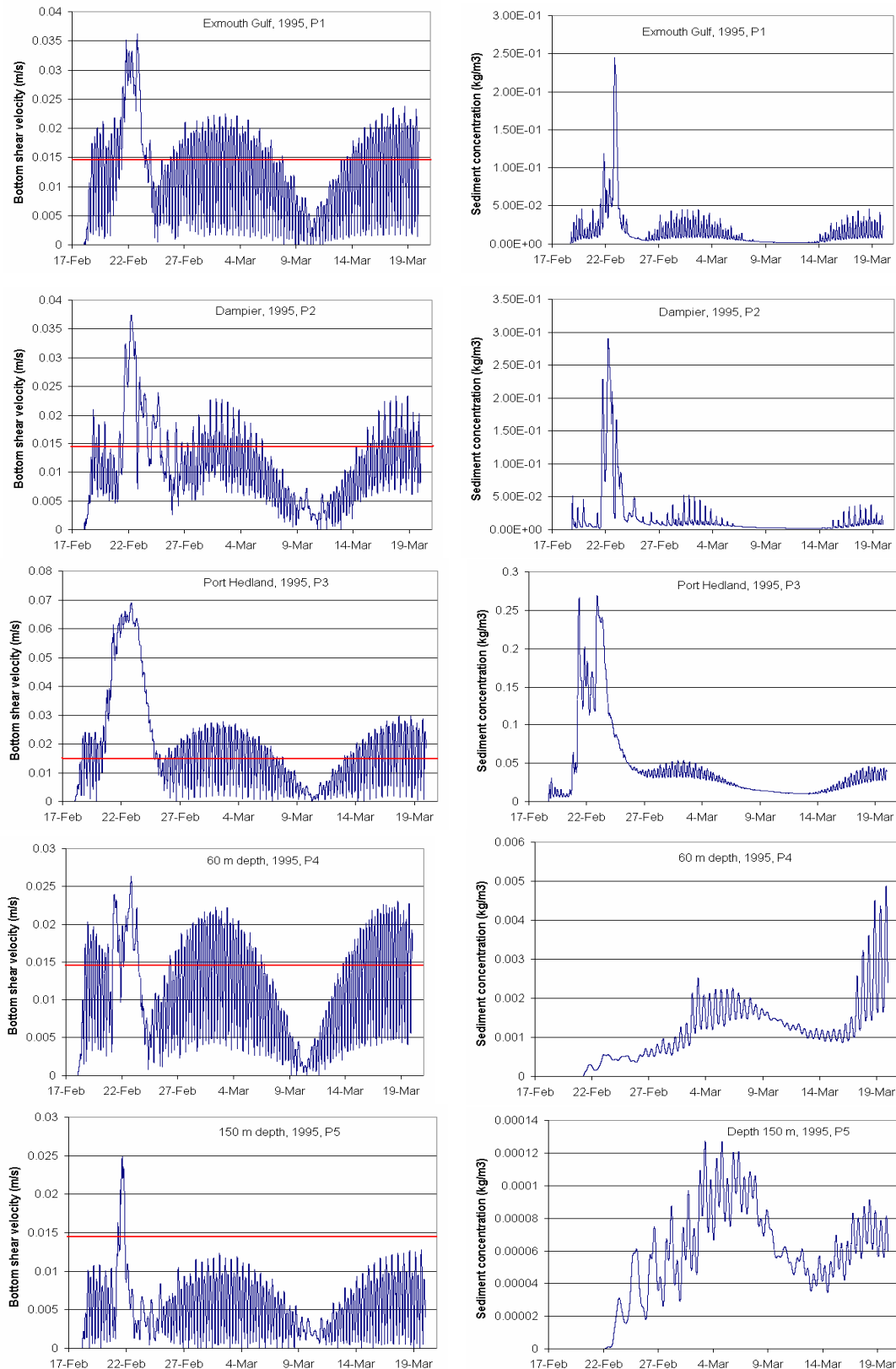
Figure 4.3.2.: Modelled bottom shear velocities (left) and surface suspended sediment concentration (right) during and after Tropical Cyclone Bobby at sites P1 in Exmouth Gulf, P2 near Dampier, P3 near Port Hedland (all at 10 m depth), and P3 (60 m) and P5 (150 m) offshore of Port Hedland (all sites are shown in figure 2.1.1). The red lines indicate the approximate bottom shear velocity threshold for resuspension for fine sediments (0.014 m s^{-1} or 0.2 N m^{-2}).
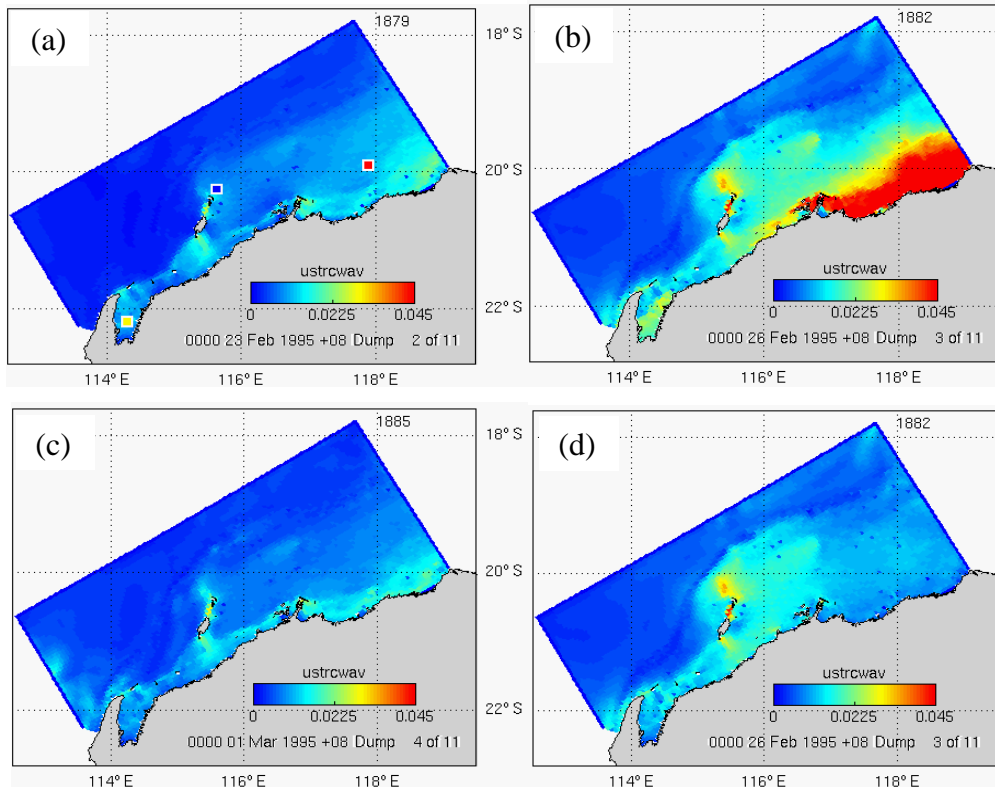
Figure 4.3.3: Shear velocities (m s^{-1}) averaged over three day periods (a) before the cyclone, (b) during the cyclone, (c) after the cyclone, and (d) during the cyclone with no waves.
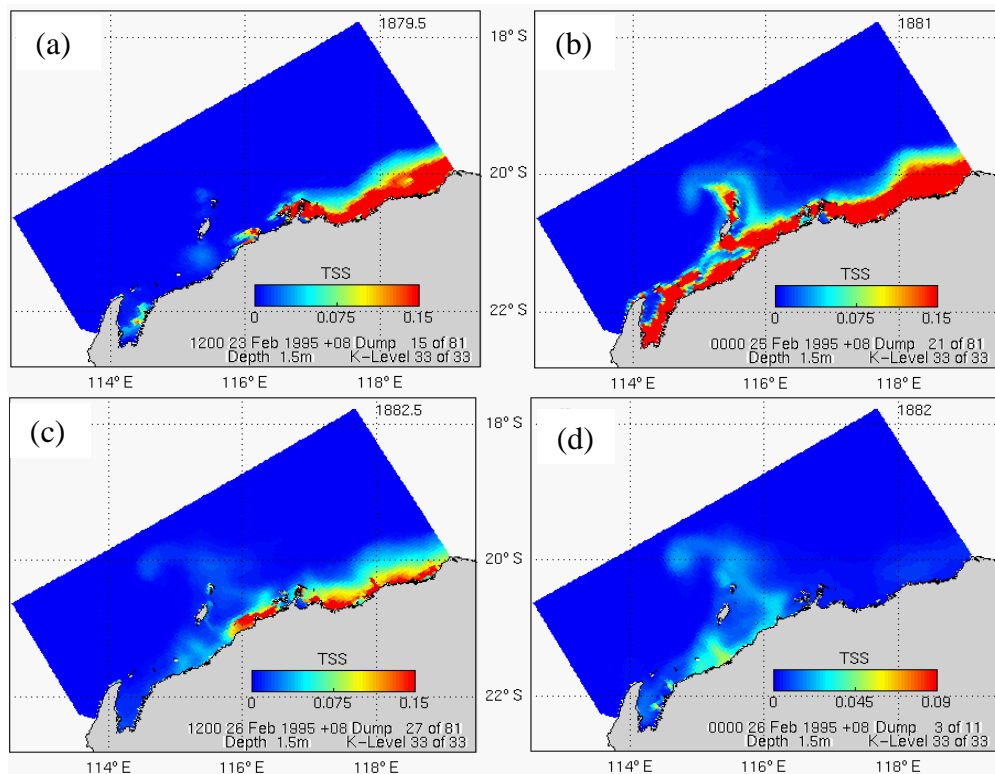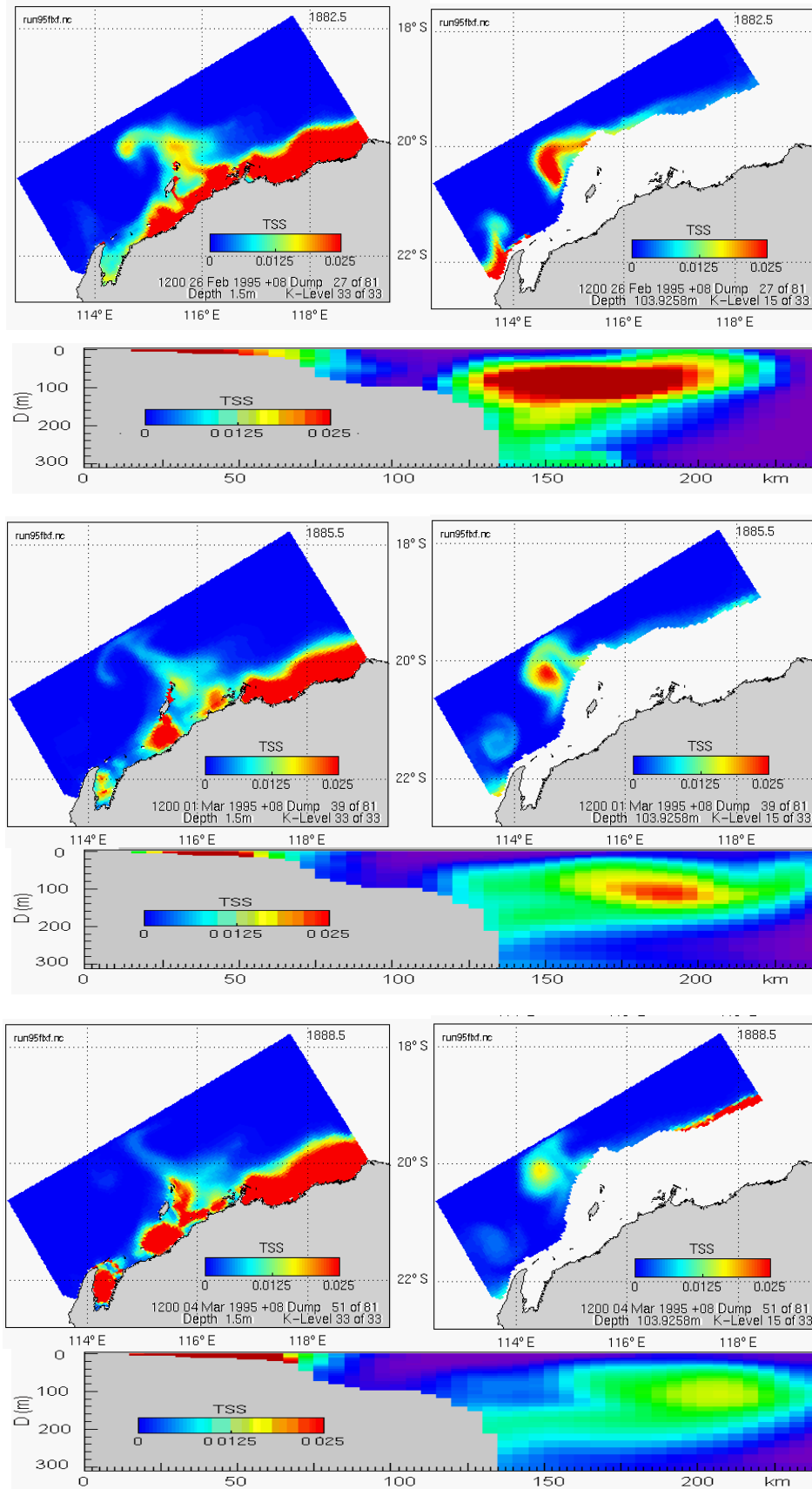

Figure 4.3.4: Surface concentrations of suspended sediments (kg m^{-3}), (a) before the cyclone, (b) during the cyclone, (c) after the cyclone, and (d) during the cyclone with no waves.
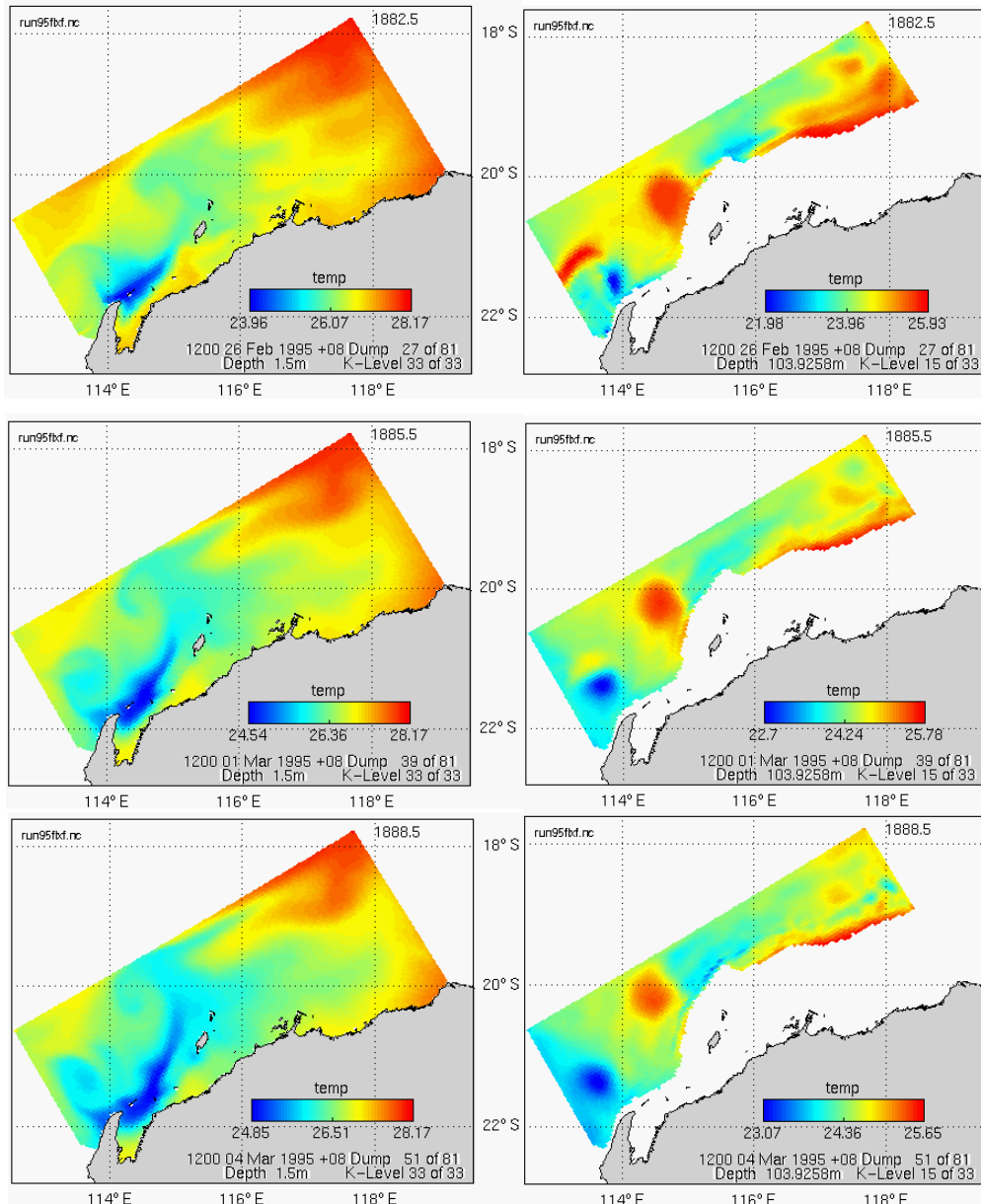
Figure 4.3.5: Modelled temperature (°C) on 26 February (top), 1 March (centre), and 4 March (bottom) at the surface (left) and at 150 m depth (right).

The net flux of all suspended sediment classes was directed offshore as the cyclone moved across the NWS, with a much smaller onshore flux as it crossed the coastline (figure 4.3.8, table 4.3.1). The alongshore flux was more variable, but predominantly to the southwest (figure 4.3.9). Peak fluxes (~2x106 kg s^{-1}) were two orders of magnitude larger than those obtained during Tropical Cyclone Olivia and three orders of magnitude larger than Tropical Cyclone Vance (figure 4.2.8). These differences are also reflected in the accumulated sediment load during Tropical Cyclone Bobby compared to the annual loads in 1996, 1998 and 1999 for both total sediment (table 4.3.1) and fine sediment fractions (tables 4.3.2). While the fluxes associated with Tropical Cyclones Olivia and Vance where clearly underestimated (due to the poor resolution of the cyclonic winds), the comparisons serve to demonstrate the very large proportion of the total load likely to be associated with cyclone events.

Figure 4.3.6: Modelled concentrations of total suspended sediment (kg m^{-3}) on February 26 (top trio), March 1 (centre trio), and March 4 (bottom trio) at the surface (left), at 150 m depth (right), and in a cross shelf section running west of Barrow Island (below).
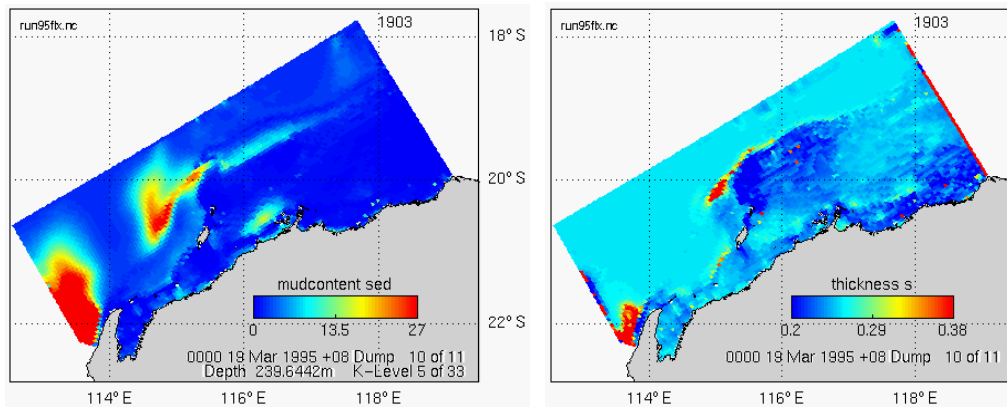
Fig 4.3.7: Modelled distribution of fine sediments on the seabed in kg m^{-3} (left) and thickness of bottom sediments in m (right) following Tropical Cyclone Bobby.
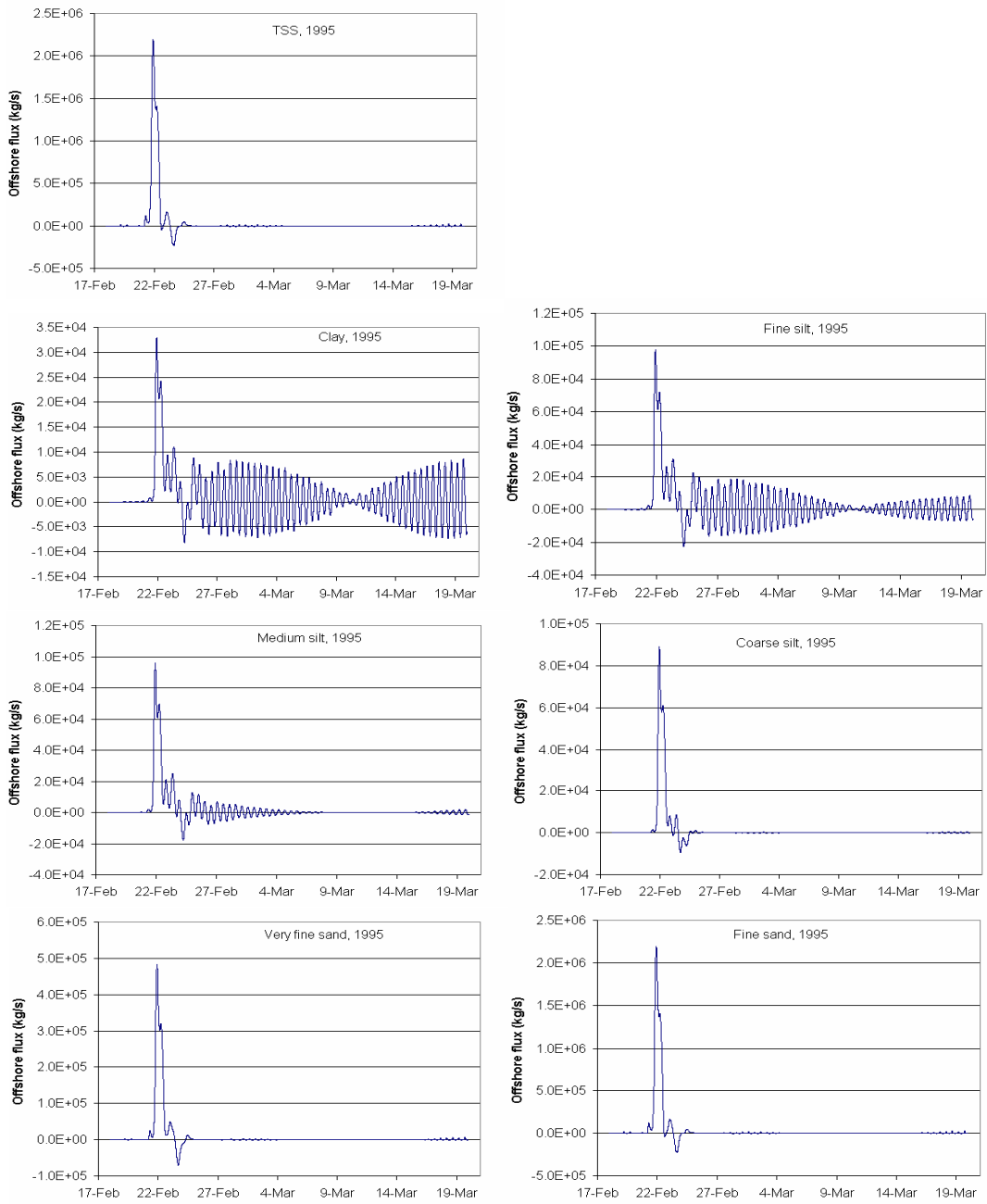
Figure 4.3.8: Modelled offshore fluxes of total suspended sediment (top) and various sediment classes during and after Tropical Cyclone Bobby. Fluxes are positive when directed into waters deeper than 150 m.

Table 4.3.1: Accumulated total sediment load on the NWS during the period affected by Tropical Cyclone Bobby (10 February to 19 March 1995) and for the years 1996, 1998, and 1999.

Period	Offshore load (kg)	Alongshore load (kg)	Balance (kg)
18/02 to 19/03 1995	136×10^9	-27×10^9	109×10^9
1996	10×10^9	-19×10^9	-9×10^9
1998	2.5×10^9	-4.9×10^9	-2.4×10^9
1999	5.6×10^9	-16×10^9	-10.4×10^9
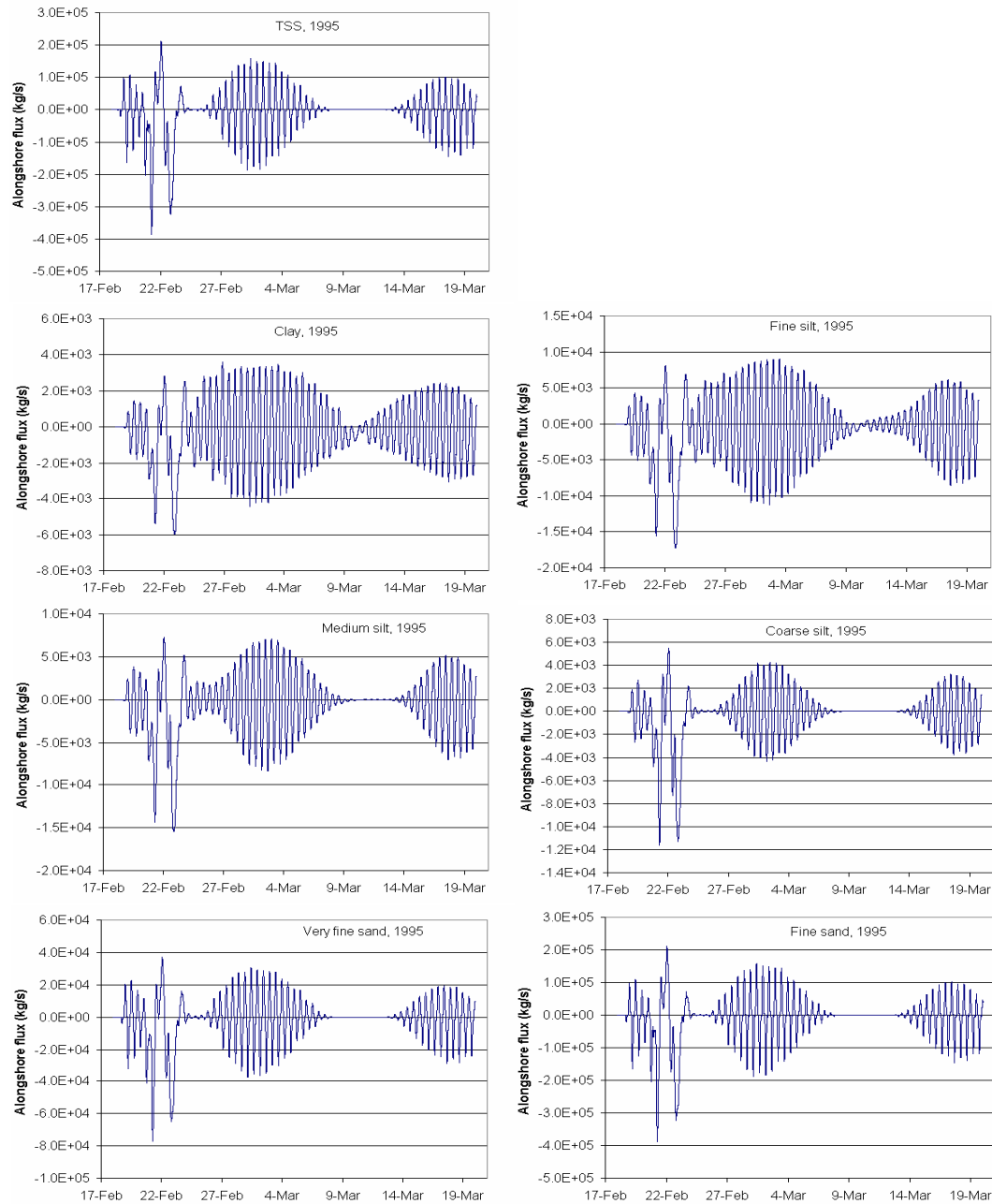
Figure 4.3.9: Modelled alongshore fluxes of total suspended sediment (top) and various sediment classes at the northeast model boundary during and after Tropical Cyclone Bobby. Fluxes are positive when directed to the northeast (i.e. out of the model domain).

Table 4.3.2: Accumulated fine sediment (silt and clay fractions) load on the NWS during the period affected by Tropical Cyclone Bobby (10 February to 19 March 1995) and for the years 1996, 1998, and 1999. The observed mean annual river load is 0.86×10^9 kg.

Period	Offshore load (kg)	Alongshore load (kg)	Balance (kg)
18/02-19/03 1995	18.0×10^9	-4.7×10^9	13.3×10^9
1996	4.8×10^9	-2.1×10^9	2.7×10^9
1998	2.2×10^9	0.7×10^9	2.7×10^9
1999	4.2×10^9	-0.7×10^9	3.5×10^9

5. CONCLUSIONS

Numerical simulations have been carried out in order to investigate sediment dynamics on the NWS from Exmouth Gulf to Port Hedland. The calculations were based on three dimensional coupled sediment transport and hydrodynamic models. The models were applied to simulate suspended sediment fluxes in 1996, 1998, and 1999, and to investigate the impact of Tropical Cyclone Bobby during February and March 1995.

The model reproduced winnowing and transportation of fine sediments in the relatively high-energy environment of the mid shelf, with active deposition restricted to localised areas. There was accumulation of fine sediments beyond the shelf break where conditions were less energetic. The transition between sediment winnowing and retention on the shelf occurred at approximately the phi3 to phi4 size class, consistent with observations (McLoughlin & Young, 1985). The model predicted a persistent strip of elevated concentrations of suspended sediment inshore, qualitatively consistent with turbidity estimates from satellite ocean colour data. Typical sediment concentrations between Dampier and Exmouth Gulf were less than 5 g m^{-3} during the neap tide and less than 10 g m^{-3} during the spring tide.

Shear stresses calculated at the mid and inner shelf regions for 1996, 1998, and 1999 frequently exceeded the threshold for fine-sediment resuspension, particularly around spring tide. However, at 150 m depth the resuspension threshold was only exceeded under extreme weather conditions. Areas of maximum resuspension were around Barrow and Monte Bello Islands, in Exmouth Gulf, and over the broad coastal and mid shore region northeast from the Dampier Archipelago.

Given the constraints in the model formulation and uncertainties in the input data, the numerical flux estimates should be considered as an indicative rather than definitive. However, they clearly demonstrate the dominant influence of the spring neap tidal cycle under most weather conditions. The longer-term offshore fluxes of fine sediments were partially balanced by an alongshore influx of sediments at the northeast boundary. However, the net flux of fine sediments at the lateral boundaries was directed offshore and exceeded the mean annual river loads by at least a factor of three. This result may indicate that these were coincidently years of sediment loss from the shelf (offsetting gains in other years); or that there are other sources of sediments not included in the model such as bank erosion; or that there are substantial errors in the flux estimates associated with factors such as boundary conditions or resuspension rates. However, such issues are only likely to be resolved through longer-term monitoring of the system.

The model also predicted major sediment transport events during tropical cyclones. For example, calculated offshore loads of fine sediments during Tropical Cyclone Bobby (13.3x10^9 kg) far exceeded annual river loads (0.86 x10^9 kg) and annual offshore loads in years without cyclones (2.7 x10^9 kg for 1998).These simulations also demonstrated the potentially important role of mesoscale structures in sediment exchange between the shelf and offshore environments. Tropical Cyclone Bobby generated a number of intense eddies along the edge of the shelf, which entrained shelf sediments and formed clouds of highly concentrated suspension. These features eventually deposited the fine sediments within highly localised patches offshore.

Sediment transport generally depends on a variety of processes, not all of which were included in the model. For example, a simplified empirical formulation was used to predict wind-wave parameters (Condie & Andrewartha, 2002). Processes such as flocculation and consolidation of fine sediments, and ripple dynamics were not simulated because of the lack of relevant observations. Only fine sediment fractions were transported, neglecting suspended and bed load transport of coarse sands. There was also a lack of data to initialise and validate the model. For example, the grain-size distribution for bottom sediments was available only for the mid to outer shelf region in the eastern half of the model domain, with very little to characterise the shallow inner shelf. No information was available on seasonal variability of the river flows or their sediment loads.

Despite the limitations in the model formulation, its predictions are broadly consistent with available observations. Given the semi-empirical nature of the model, its complexity is compatible with the quality of the available measurements. Further progress in sediment modelling on the NWS should be based on extended data sets for sediment processes, such as grain size distributions, flocculation, consolidation, river loads, and improved wind and wave products.

REFERENCES

Brunskill G., A. Orpin, I. Zagorskis, K. Woolfe, J. Ellison (2001) Geochemistry and particle size of surface sediments of Exmouth Gulf, Northwest Shelf, Australia. Cont. Shelf Res., 21, 157-201.

Bruce, B.D., S. A. Condie, and C. A. Sutton (2001) Larval distribution of blue grenadier (Macruronus novaezelandiae Hector) in south-eastern Australia: further evidence for a second spawning area. Mar. Freshwat. Res., 52: 603-610.

Burns, K.A., J.K. Volkman, J. Cavanagh and D. Brinkman (2003) Lipids as biomarkers for carbon cycling on the Northwest Shelf of Australia: results from a sediment trap study. Mar. Chem., 80, 103-128.

Coastal Engineering Manual, Part III. (1999) U.S. Army Corps of Engineers. Washington, DC 20314-1000.

Condie, S.A., J. Andrewartha, J. Mansbridge, and J. Waring (2006) Modelling Circulation and Connectivity on Australia's North West Shelf. NWSJEMS Technical Report No. 6 CSIRO Marine and Atmospheric Research.

Condie, S.A. and J. Andrewartha (2002) North West Shelf Joint Environmental Management Study: Milestone Report No. 2.2: Wave Modelling. CSIRO Marine Research Report.

Condie, S.A., Loneragan, N.R., and Die, D.J. (1999) Modelling the recruitment of tiger prawns (Penaeus esculentus and P. semisulcatus) to nursery grounds in the Gulf of Carpentaria, northern Australia: implications for assessing stock-recruitment relationships. Mar. Ecol. Prog. Ser., 178: 55-68.

Cresswell, G.R., Frische, A., Peterson, J., and Quadfasel, D. (1993) Circulation in the Timor Sea. J. Geophys. Res., 98, 14379-14389.

Drake D. (1977) Suspended sediment transport and mud deposition on continental shelves. In: Marine sediment transport and environmental management. Ed by Stanley D., and Swift D.,Wiley-Interscience Publication., pp 127-158.

Fandry, C. B. and R. K. Steedman (1994) Modelling the dynamics of the transient, barotropic response of continental shelf waters to tropical cyclones. Cont. Shelf Res., 14, 1723-1750.

Godfrey, J.S. and Ridgway, K.R. (1985) The large-scale environment of the poleward-flowing Leeuwin Current, Western Australia: Longshore steric height gradients, wind stresses and geostrophic flow. J. Phys. Oceanogr., 15, 481-495.

Grant, W. D. and O. S. Madsen (1979) Combined wave and current interaction with a rough bottom. J. Geophys. Res., 84, 1797-1808.

Hamilton, L. J. (1997) Methods to obtain representative surface wave spectra, illustrated for two ports of north-western Australia. Mar. Freshwater Res., 48, 43-57.

Harris P.T., Smith R., Anderson O., Coleman R., Greenslade D. (2000) GEOMAT – Modelling of Continental Shelf Sediment Mobility in Support of Australia's regional Marine Planning Process. AGSO Report record No. 2000/XX.

Hearn, C.J. and P. E. Holloway (1990) A three dimensional barotropic model of the response of the Australian North West Shelf to tropical cyclones. J. Phys. Oceanogr., 20, 60-80.

Herzfeld M, J. Parslow, P. Sakov, and J. Andewartha (2006) Biogeochemical modelling on Australia's North West Shelf. NWSJEMS Technical Report No. 8. CSIRO Marine and Atmospheric Research.

Herzfeld, M., J. Waring, J. Parslow, N. Margvelashvili, P. Sakov and J. Andrewartha (2002) MECO, Model of Estuarine and Coastal Oceans, V4.0, Scientific Manual, CSIRO Marine Research.

Heyward A.J., Revill A.T., Sherwood C.R. (2006). Review of Research and Data Relevant to Marine Environmental Management of Australia's North West Shelf. NWSJEMS Technical Report No. 1. CSIRO Marine and Atmospheric Research.

Holland, G.J. (1980) An analytic model of the wind and pressure profiles in Hurricanes. Mon. Weather. Rev., 108, 1212-1218.

Holloway, P.E. (1985) A comparison of semidiurnal internal tides from different bathymetric locations on the Australian North West shelf. J. Phys. Oceanogr., 15, 240-251.

Holloway, P.E. (1995) Leeuwin Current observations on the Australian North West Shelf, May-June 1993. Deep Sea Res., 42, 285-305.

Holloway, P. E. (1996) A numerical model of internal tides with application to the Australian North West Shelf. J. Phys. Oceanogr., 21-37.

Holloway, P.E. (2001) A regional model of the semidiurnal internal tide on the Australian North West Shelf. J. Geophys. Res., 106, 19625-19638.

Holloway, P. E. and H. C. Nye (1985) Leeuwin Current and wind distributions on the southern part of the Australian North West Shelf between January 1982 and July 1983. Aust. J. Mar. Freshwat. Res., 36, 123-137.

Jones, H.A. (1973) Marine Geology of the Northwest Australian continental shelf. BMR Bull. 136.

Kalnay, E., M. Kanamitsu, R. Kistler, W. Collins, D. Deaven, L. Gandin, M. Iredell, S. Saha, G. White, J. Woollen, Y. Zhu, M. Chelliah, W. Ebisuzaki, W. Higgins, J. Janowiak, K.C. Mo, C. Ropelewski, J. Wang, A. Leetmaa, R. Reynolds, R. Jenne and D. Joseph (1996) The NCEP/NCAR 40-year re-analysis project. Bull. Amer. Meteor. Soc., 77, 437-471.

Lough, J.M. (1998) Coastal climate of northwest Australia and comparisons with the Great Barrier Reef: 1960 to 1992. Coral Reefs, 17, 351-367.

Margvelashvili, N. (2003) MECOSED Scientific Manual. CSIRO Marine Research.

McLoughlin, R.J. and P.C. Young, (1985) Sedimentary provinces of the fishing grounds of the North West Shelf of Australia: grain-size frequency analysis of surficial sediments. Aust. J. Mar. Freshwat. Res., 36, 671–681.

McLoughlin, R.J., Davis, T.L.O. & Ward, T.J., (1988) Sedimentary provinces, and associated bedforms and benthos on the Scott Reef–Rowley Shoals platform off north west Australia. Australian Journal of Marine and Freshwater Research, 39(2): 133–144.

Ribbe J. and P. Holloway (2001) A model of suspended sediment transport by internal tides. Cont. Shelf Res., 21, 395-422.

Ruprecht, J.K. and Ivansecu, S. (1996). Surface hydrology of the Pilbara region. Water and Rivers Commission (unpublished report).

SeaWiFS Technical Report (1997) Case Studies for SeaWIFS Calibration and Validation, Part 4. Vol. 41, Ch. 2.

Schiller, A., J. S. Godfrey, P. C. McIntosh, G. Meyers, and R. Fiedler (2000) Interannual dynamics and thermodynamics of the Indo-Pacific Oceans. J. Phys. Oceanogr., 30, 987-1012.

Semeniuk, V., P. N. Charmer and I. Le Provost (1982) The marine environments of the Dampier Archipelago. J. Roy. Soc. West. Aust., 65, 97-114.

Sherwood C.R. (1998) Estimates of bottom Stress on the North West Shelf of Australia. CSIRO DMR Report No. OMR-109/116, 19 pp.

U.S. Army Coastal Engineering Research Center (1984) Shore Protection Manual. U.S. Government Printing Office.

Walker, S. J. (1999) Coupled hydrodynamic and transport models of Port Phillip Bay, a semi-enclosed bay in south-eastern Australia. Mar. Freshwat. Res., 50: 469-481.

Webster, I. (1985) Wind-driven circulation on the North West Shelf of Australia. J. Phys. Oceanogr., 15, 1357-1368.

ACKNOWLEDGMENTS

Andrew Heyward
Barry Hutchins
Bryan Jenkins
Di Jones
Ian LeProvost
Ray Masini
Mike Moran
Steve Newman
Eric Paling
Kelly Pendoley
Bob Prinz
Chris Simpson
Shirley Slack-Smith
Di Walker

Reviewers
Peter Craig
Frederick Saint-Cast
Chris Fandry

Editorial and publishing
Louise Bell – Graphics/cover design
Lea Crosswell – Webpage design
Rob McKenzie – Editor
Diana Reale – Webpage design
Linda Thomas – Editorial consultant/layout and design
Helen Webb – Editorial consultant/Project Manager

Front cover photos courtesy of:
Centre – Coral reef ecosystem, WA Museum, Clay Bryce
Aquaculture pearls, Department of Fisheries WA
Recreational fishing, Department of Fisheries WA, Jirri Lockman
Offshore petroleum platform, Woodside Energy Ltd
Commercial Fishing, Department of Fisheries WA
Tourism, CSIRO
Coastal development aerial photos, Hamersley Iron Pty Ltd